iScience

CellPress
OPEN ACCESS

Article

D-Tryptophan suppresses enteric pathogen and pathobionts and prevents colitis by modulating microbial tryptophan metabolism

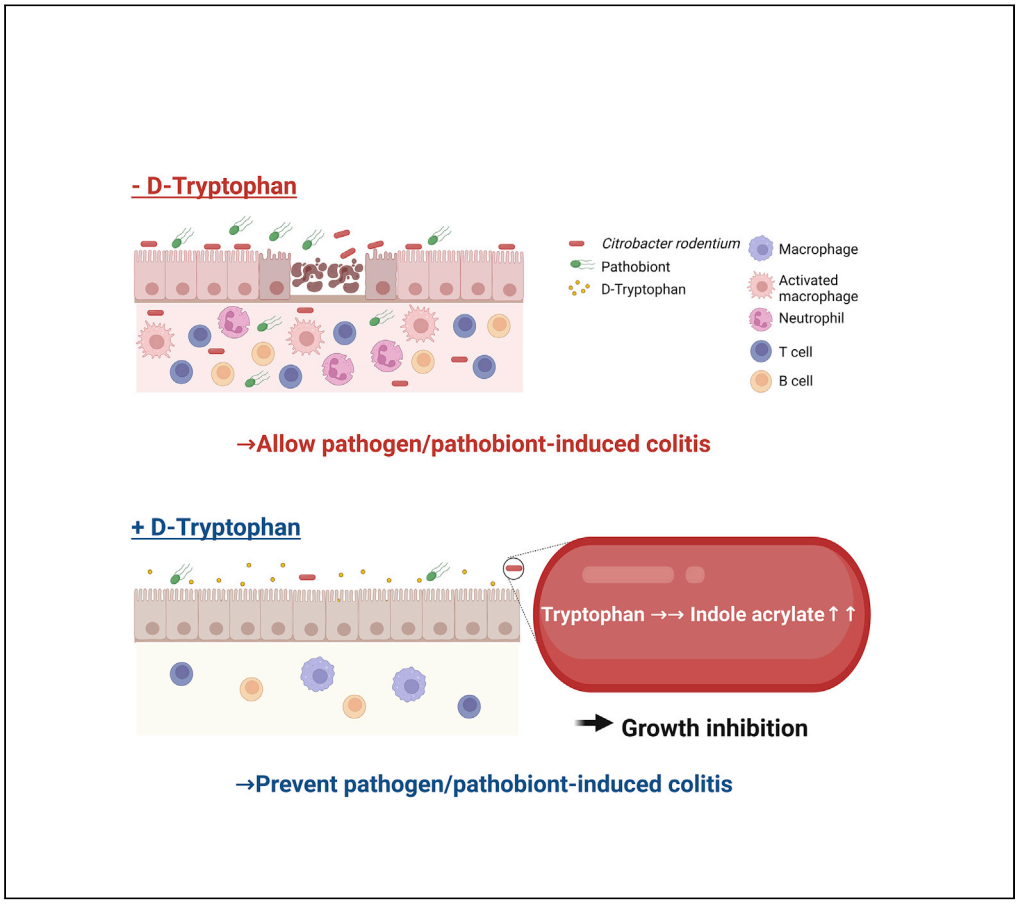

Natsumi Seki, Tatsuki Kimizuka, Monica Gondo, ..., Makoto Suematsu, Koji Hase, Yun-Gi Kim

ykim@keio.jp

Highlights

D-Trp inhibits the growth of *Citrobacter rodentium in vitro* and *in vivo*

D-Trp suppresses experimental colitis by the depletion of specific gut microbes

IA is the metabolite that determines the susceptibility of enteric microbes to D-Trp

Seki et al., iScience 25, 104838
August 19, 2022
https://doi.org/10.1016/j.isci.2022.104838

iScience

CellPress
OPEN ACCESS

Article

D-Tryptophan suppresses enteric pathogen and pathobionts and prevents colitis by modulating microbial tryptophan metabolism

Natsumi Seki,[1,2,6] Tatsuki Kimizuka,[1,2,6] Monica Gondo,[1,2,6] Genki Yamaguchi,[1,2,6] Yuki Sugiura,[3] Masahiro Akiyama,[1] Kyosuke Yakabe,[1,2] Jun Uchiyama,[1,2] Seiichiro Higashi,[4] Takeshi Haneda,[5] Makoto Suematsu,[3] Koji Hase,[2] and Yun-Gi Kim[1,7,*]

SUMMARY

D-Amino acids (D-AAs) have various functions in mammals and microbes. D-AAs are produced by gut microbiota and can act as potent bactericidal molecules. Thus, D-AAs regulate the ecological niche of the intestine; however, the actual impacts of D-AAs in the gut remain unknown. In this study, we show that D-Tryptophan (D-Trp) inhibits the growth of enteric pathogen and colitogenic pathobionts. The growth of *Citrobacter rodentium in vitro* is strongly inhibited by D-Trp treatment. Moreover, D-Trp protects mice from lethal *C. rodentium* infection via reduction of the pathogen. Additionally, D-Trp prevents the development of experimental colitis by the depletion of specific microbes in the intestine. D-Trp increases the intracellular level of indole acrylic acid (IA), a key molecule that determines the susceptibility of enteric microbes to D-Trp. Treatment with IA improves the survival of mice infected with *C. rodentium*. Hence, D-Trp could act as a gut environmental modulator that regulates intestinal homeostasis.

INTRODUCTION

L-Amino acids are essential for all forms of life as they act as the building blocks of proteins, including enzymes, antibodies, and hormones. In contrast, D-amino acids (D-AAs), the enantiomeric counterparts of L-amino acids, have long been considered non-functional. Earlier studies did not typically observe their presence in organisms. However, accumulating evidence suggests that D-AAs, such as D-Serine, D-Aspartate, D-Alanine, and D-Cysteine, are present in mammalian tissues (Kiriyama and Nochi, 2016) and play important roles in numerous physiological processes in the human body (D'Aniello, 2007; Hashimoto et al., 1992; Homma, 2007; Mori and Inoue, 2010).

D-AAs are critical constituents of peptidoglycan, an essential component of the bacterial cell wall (Hancock, 1960; Park and Strominger, 1957). Furthermore, diverse bacterial species are known to produce and release different sets of D-AAs to the environment in millimolar range concentrations (Lam et al., 2009). For instance, gut microbiota increases free D-AA levels in the intestine (Matsumoto et al., 2018; Sasabe et al., 2016). These D-AAs function as potent bactericidal molecules. Such molecules act directly or their action is mediated by host D-amino acid oxidase (DAO) (Alvarez et al., 2018; Sasabe et al., 2016). These D-AAs may have the ability to regulate microbial communities (Cava et al., 2011; Kolodkin-Gal et al., 2010).

Some symbiotic microorganisms in the intestine act as pathogens under certain conditions, usually involving environmental and/or genetic alterations (Dianda et al., 1997; Sellon et al., 1998; Taurog et al., 1994). Such resident microbes with pathogenic potential are referred to as pathobionts (Honda and Littman, 2012). Pathobionts are innocuous to the host under normal conditions but an imbalanced state of the gut microbiota, triggered by inherent immune defects as well as changes in diet and/or acute inflammation, induces the proliferation of the pathobionts and triggers intestinal inflammation (Devkota et al., 2012; Garrett et al., 2007). Certain pathogens have also developed strategies to promote their replication in the presence of the gut microbiota. Indeed, some pathogens within the family Enterobacteriaceae, such as *Citrobacter rodentium*, initially utilize virulence factors to induce intestinal inflammation, which is advantageous for the bacterial growth in the intestinal lumen (Barman et al., 2008; Kamada et al., 2012;

[1]Research Center for Drug Discovery, Faculty of Pharmacy and Graduate School of Pharmaceutical Sciences, Keio University, Tokyo 105-8512, Japan

[2]Department of Biochemistry, Faculty of Pharmacy and Graduate School of Pharmaceutical Sciences, Keio University, Tokyo 105-8512, Japan

[3]Department of Biochemistry, Keio University School of Medicine, Tokyo 160-8582, Japan

[4]Co-Creation Center, Meiji Holdings Co., Ltd., 1-29-1 Nanakuni, Hachiouji, Tokyo 192-0919, Japan

[5]Laboratory of Microbiology, School of Pharmacy, Kitasato University, Tokyo 108-8641, Japan

[6]These authors contributed equally

[7]Lead contact

*Correspondence: ykim@keio.jp

https://doi.org/10.1016/j.isci.2022.104838

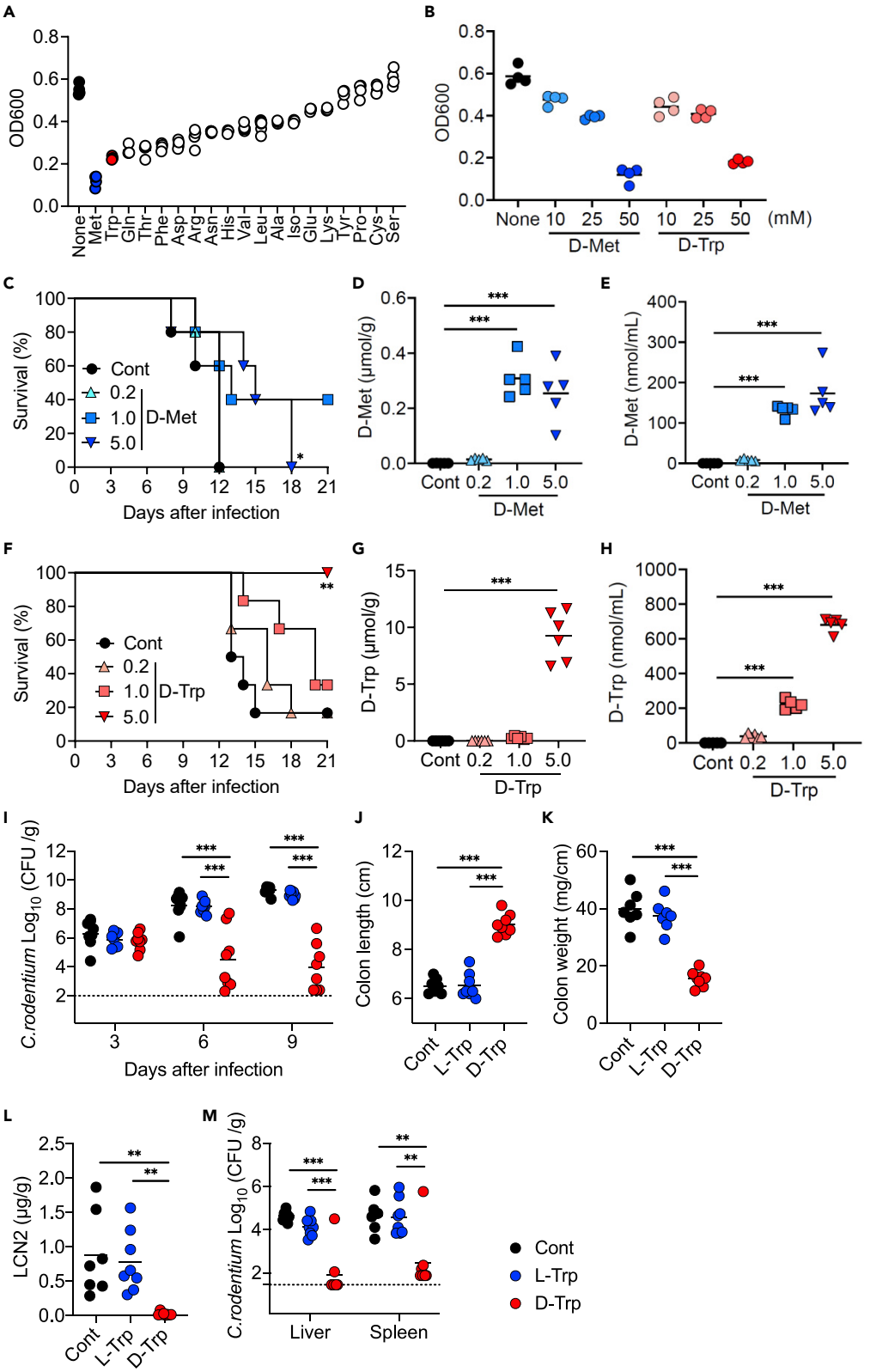
A
OD600
None Met Trp Gln Thr Phe Asp Arg Asn His Val Leu Ala Iso Glu Lys Tyr Pro Cys Ser
B
OD600
None 10 25 50 10 25 50 (mM)
D-Met
D-Trp
C
Survival (%)
Cont
0.2
1.0
5.0
D-Met
Days after infection
D
D-Met (μmol/g)
Cont 0.2 1.0 5.0
D-Met
E
D-Met (nmol/mL)
Cont 0.2 1.0 5.0
D-Met
F
Survival (%)
Cont
0.2
1.0
5.0
D-Trp
Days after infection
G
D-Trp (μmol/g)
Cont 0.2 1.0 5.0
D-Trp
H
D-Trp (nmol/mL)
Cont 0.2 1.0 5.0
D-Trp
I
C.rodentium Log10 (CFU /g)
Days after infection
J
Colon length (cm)
Cont L-Trp D-Trp
K
Colon weight (mg/cm)
Cont L-Trp D-Trp
L
LCN2 (μg/g)
Cont L-Trp D-Trp
M
C.rodentium Log10 (CFU /g)
Liver Spleen
Cont
L-Trp
D-Trp

Figure 1. Effects of $_{D}$-Tryptophan on the growth of enteric pathogen

(A and B) Optical density (OD) measured at 600 nm after culturing *Citrobacter rodentium* in LB broth supplemented with or without 50 mM of each $_{D}$-amino acid (A) (n = 4 samples per group) or with or without various concentrations of $_{D}$-Methionine ($_{D}$-Met) or $_{D}$-Tryptophan ($_{D}$-Trp) (B) (n = 4 samples per group) for 24 h.

(C-H) Mice were fed chow diets supplemented with $_{D}$-Methionine ($_{D}$-Met) or $_{D}$-Tryptophan ($_{D}$-Trp) at concentrations of 0% (Control; Cont), 0.2%, 1%, or 5% and then infected orally with 2×10^{9} colony-forming units (CFU) of *C. rodentium* (n = 5-6 mice per group). The mice were fed with their respective diets beginning 10 days before infection and continuing through the end of the experiment.

(C and F) Survival rates for 21 days after infection with *C. rodentium*.

(D, E, G, H) $_{D}$-Trp levels in (D and G) feces and (E and H) plasma derived from mice fed supplemented chow diets for 10 days before the infection.

(I-M) Mice were fed with the respective diets (Cont, unsupplemented diet; $_{L}$-Trp, 5% $_{L}$-Tryptophan supplemented diet; $_{D}$-Trp, 5% $_{D}$-Tryptophan supplemented diet) and then infected orally with 2×10^{9} CFU of *C. rodentium* (n = 7-8 mice per group). The mice were fed their respective diets beginning 2 weeks before infection and continuing through the end of the experiment.

(I) Fecal *C. rodentium* load on days 3, 6, and 9 post-infection.

(J) Colon length and (K) colon weight per cm on day 10 post-infection.

(L) Fecal Lipocalin-2 (LCN2) concentration on day 9 post-infection.

(M) *C. rodentium* load in the liver and the spleen at day 10 post-infection.

Each dot represents one sample or mouse. Horizontal bars indicate mean values. Statistical significance was assessed using the Log-rank test in panels C and F, one-way ANOVA with Dunnett's multiple comparison test in panels D, E, G, and H, and Tukey's multiple comparison test in panels I, J, K, L, and M. *$p < 0.05$; **$p < 0.01$; ***$p < 0.001$. All the experiments were conducted at least three independent times.

Lupp et al., 2007). Therefore, the inhibition of the growth of pathogens or indigenous pathobionts is critical for controlling enteric infection and intestinal inflammation.

The influence of $_{D}$-AAs on gut microbial communities and environments is primarily unknown. We hypothesized that certain $_{D}$-AAs could maintain gut homeostasis by controlling the growth of enteric pathogens and/or pathobionts. In the present study, we assessed whether specific $_{D}$-AA influences the growth of enteric pathogens and pathobionts, and changes the composition of gut microbial communities, thereby suppressing microbially induced colitis. Furthermore, we identified how this $_{D}$-AA inhibited the growth of colitogenic gut microbes.

RESULTS

$_{D}$-Tryptophan inhibits the growth of enteric pathogen

We first examined the inhibitory effects of $_{D}$-AAs on the growth of the enteric pathogen *in vitro*. Compared to the untreated control, treatment with most $_{D}$-AAs, particularly $_{D}$-Methionine ($_{D}$-Met) and $_{D}$-Trp, inhibited the growth of *C. rodentium*, a natural pathogen of mice, which are used to model human infections with enteropathogenic *Escherichia coli* in a dose-dependent manner (Borenshtein et al., 2008) (Figures 1A and 1B). We then assessed whether $_{D}$-Met and $_{D}$-Trp, which were the strongest growth inhibitory effect on *C. rodentium in vitro*, can inhibit enteric pathogen infection *in vivo*. Treatment with $_{D}$-Met protected the mice modestly from lethal infection with *C. rodentium* (Figure 1C). Fecal and plasma $_{D}$-Met levels were increased when a high dose of $_{D}$-Met was administered orally (Figures 1D and 1E). Treatment with $_{D}$-Trp remarkably improved the survival of *C. rodentium*-infected mice in a dose-dependent manner (Figure 1F). Food intake was decreased for a couple of days and body weight was lower in the mice treated with 5% $_{D}$-Trp compared with other groups before the infection. However, food intake and body weight, eventually, became comparable among all the groups during the infection (Figures S1A-S1D). Fecal and plasma $_{D}$-Trp levels were significantly increased in the mice treated with 5% $_{D}$-Trp (Figures 1G and 1H). We next determined whether $_{D}$-Trp can inhibit the growth of *C. rodentium* in the gut. *C. rodentium* was detected in the feces of inoculated mice 3 days post-infection, and the burden of *C. rodentium* further increased and remained elevated up to days 6 and 9. Treatment with $_{D}$-Trp, but not $_{L}$-Trp, reduced the pathogen load from day 6, and the fecal numbers of *C. rodentium* remained low until day 9 after the infection (Figure 1I). The mice treated with $_{D}$-Trp had significantly longer colon length and lower colon weight compared with those of the control and $_{L}$-Trp-treated mice (Figures 1J and 1K). Fecal concentrations of lipocalin-2, a fecal marker for colitis severity, increased in *C. rodentium*-infected mice. Lipocalin-2 concentrations were strongly suppressed by treatment with $_{D}$-Trp but not with $_{L}$-Trp (Figure 1L). Pretreatment with $_{L}$-Trp or $_{D}$-Trp before the infection did not increase the fecal level of lipocalin-2 (Figure S1E). We also observed a higher burden of *C. rodentium* in the livers and spleens of infected untreated mice and mice treated with $_{L}$-Trp.

However, we detected a lower number of pathogens in the livers and spleens of D-Trp-treated mice nine days post-infection (Figure 1M). The gut microbiota metabolize tryptophan into metabolites that act as aryl hydrocarbon receptor (AhR) ligands (Agus et al., 2018). AhR-deficient mice exhibit a high pathogen burden and are susceptible to *C. rodentium* infection (Qiu et al., 2012). Thus, D-Trp could activate AhR which contributes to the protection of mice against *C. rodentium* infection. Therefore, we next compared the ability of L-Trp and D-Trp to activate AhR. Treatment with D-Trp as well as L-Trp strongly enhanced the expression of *Cyp1a1*, an AhR target gene, but the expression level was comparable in both treatment groups (Figure S2A). On the other hand, the expression of Reg3γ, another AhR target gene, was neither upregulated by D-Trp or L-Trp (Figure S2B). Therefore, the activation of AhR by D-Trp may not contribute to protecting the mice from *C. rodentium* infection. Collectively, these results indicate that D-Trp inhibits the growth of enteric pathogen.

D-Tryptophan suppresses experimental colitis by influencing the growth and composition of gut microbiota

We next assessed whether D-Trp can also influence the growth and composition of gut microbiota. We used two mouse colitis models in which severities were strongly influenced by microbiota composition (Feng et al., 2010; Hernandez-Chirlaque et al., 2016; Reinoso Webb et al., 2018). We first induced acute colitis by the oral administration of dextran sulfate sodium (DSS). Induction of acute colitis is mediated primarily by effectors of innate immunity and causes damage to the epithelial barrier and results in significant weight loss and appearance of pathological symptoms such as colon shortening (te Velde et al., 2007). The highest weight loss was observed in untreated and L-Trp-pretreated mice administered with DSS, while the bodyweight of D-Trp-pretreated mice remained almost unchanged (Figure 2A and S3A). Consistent with this result, D-Trp-pretreated mice showed lower colon weight and exhibited less inflammation in the colon upon DSS administration than untreated mice (Figures 2B-2D). In addition, the percentage of neutrophils ($CD45^+CD11b^+Ly6G^+$), inflammatory monocytes ($CD45^+CD11b^+F4/80^+$ $SiglecF^-Ly6C^+$), and B cells ($CD45^+B220^+TCR\beta^-$) was lower, but that of T cells ($CD45^+CD4^+TCR\beta^+$) was higher, in the colonic tissues derived from D-Trp-pretreated mice than those from untreated mice following DSS administration (Figures 2E-2H). Pretreatment with L-Trp or D-Trp neither influenced body weight changes nor induced apparent inflammation and the percentage of immune cells was comparable compared with the untreated group, as assessed by flow cytometry (Figures S3B and S3C). These results indicate that pretreatment with D-Trp suppresses gut microbiota-induced colitis. We also assessed the therapeutic effects of D-Trp on DSS-induced colitis. After the administration of DSS for 5 days, the mice were treated with D-Trp, and changes in the body weight were monitored. Untreated mice were used as the control. D-Trp treatment resulted in a significantly lower loss of bodyweight and longer colon length compared to that observed in the control (Figures S4A and S4B).

We next induced chronic colitis by adoptive transfer of $CD4^+CD25^-$ T cells into *Rag1*$^{-/-}$ recipients, which resulted in epithelial hyperplasia, goblet cell depletion, and transmural inflammation, thereby increasing the ratio of colon weight/length (Harris et al., 2009). The mice treated with D-Trp had significantly longer colon length and lower colon weight compared with those of the control and L-Trp-treated mice (Figures S5A and S5B). In line with this finding, inflammation was observed in the colons of untreated- and L-Trp-treated mice as shown by higher histological scores, while D-Trp-treated mice did not demonstrate detectable inflammation 3 weeks after the adoptive transfer (Figures S5C and S5D). In addition, the expressions of inflammatory cytokines, including *Tnf*, *Il1b*, and *Il6*, were higher in the colonic tissues derived from untreated- and L-Trp-treated mice than those of D-Trp-treated mice (Figure S5E).

Based on these results, we presumed that treatment with D-Trp alters the microbial composition in the distal gut and exerts anti-colitogenic effects. Therefore, we next assessed whether treatment with D-Trp influences the gut microbial communities. The 16S ribosomal RNA gene sequencing revealed that treatment with D-Trp changed the composition of the fecal microbiota, as shown by principal component analysis (Figure 3A). Mice treated with D-Trp showed an increased abundance of bacteria belonging to the family Lactobacillaceae, Tannerellaceae, and Bacteroidaceae, and decreased abundance of bacteria belonging to the families Lachnospiraceae, Muribaculaceae, and Rikenellaceae (Figures 3B and 3C). Treatment with D-Trp did not alter the total bacterial number in the feces (Figure 3D). We then assessed whether the gut microbiota altered by D-Trp treatment is sufficient to prevent colitis development. Germ-free (GF) mice colonized with the gut microbiota derived from the control or D-Trp-treated mice were administered with DSS, followed by a comparison of weight changes. The gut microbiota from each group was successfully transferred into GF mice, as confirmed by 16S rRNA gene and principal component analysis (Figures

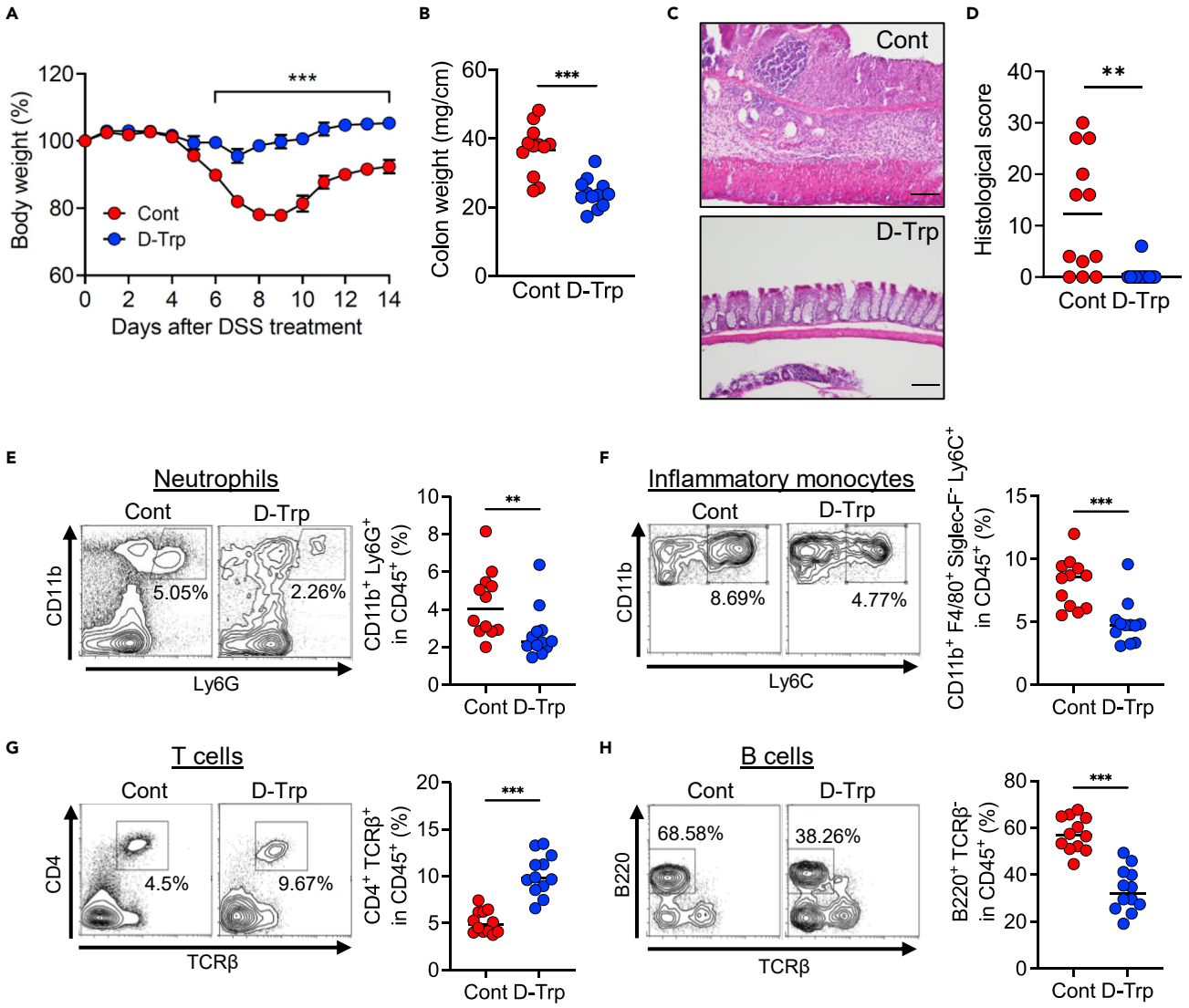

Figure 2. Protective effect of D-Tryptophan against experimental colitis

(A-H) Acute colitis was induced in SPF wild-type mice via treatment with 2% dextran sulfate sodium (DSS) for 5 days, followed by providing plain water for 9 days. The mice were treated orally every day with 1 mL of 0.5% carboxymethyl cellulose (CMC) or 5% D-Tryptophan suspended in 0.5% CMC beginning 1 week before DSS treatment and continuing through the end of the experiment (n = 12 mice per group). The mice were euthanized, and the colon was harvested 9 days following DSS treatment (B-H).

(A) Changes in body weight over 14 days.

(B) Colon weight per cm.

(C) Representative hematoxylin and eosin-stained colonic sections (scale bar: 100 μm).

(D) Histological score.

(E-H) Representative flow cytometry plots and numbers of (E) $CD45^+CD11b^+Ly6G^+$ cells (Neutrophils), (F) $CD45^+CD11b^+F4/80^+Siglec\text{-}F^-Ly6C^+$ cells (Inflammatory monocytes), (G) $CD45^+CD4^+TCR\beta^+$ cells (T helper cells), and (H) $CD45^+B220^+TCR\beta^-$ cells (B cells) in the colonic lamina propria. Each dot represents one mouse or the mean ± SEM. Horizontal bars indicate mean values. Statistical significance was assessed using unpaired Student's *t* test in panels E, F, G, and H, Welch's *t*-test in panels B and D, and two-way ANOVA with Šidák corrections for multiple comparisons in panel A. *p < 0.05; **p < 0.01; ***p < 0.001; N.S., not significant. All the experiments were conducted at least three independent times.

S6A and S6B). Weight loss was observed in DSS-treated GF mice colonized with the gut microbiota derived from control mice. The weight loss of GF mice colonized with the gut microbiota derived from D-Trp-treated mice was significantly suppressed (Figure S6C). These results demonstrate that D-Trp affects gut microbiota composition and directly reduces the number of colitogenic bacteria. We then examined whether each gut microbe showed differential susceptibilities to D-Trp. *Lactobacillus spp.* and *Bacteroides*

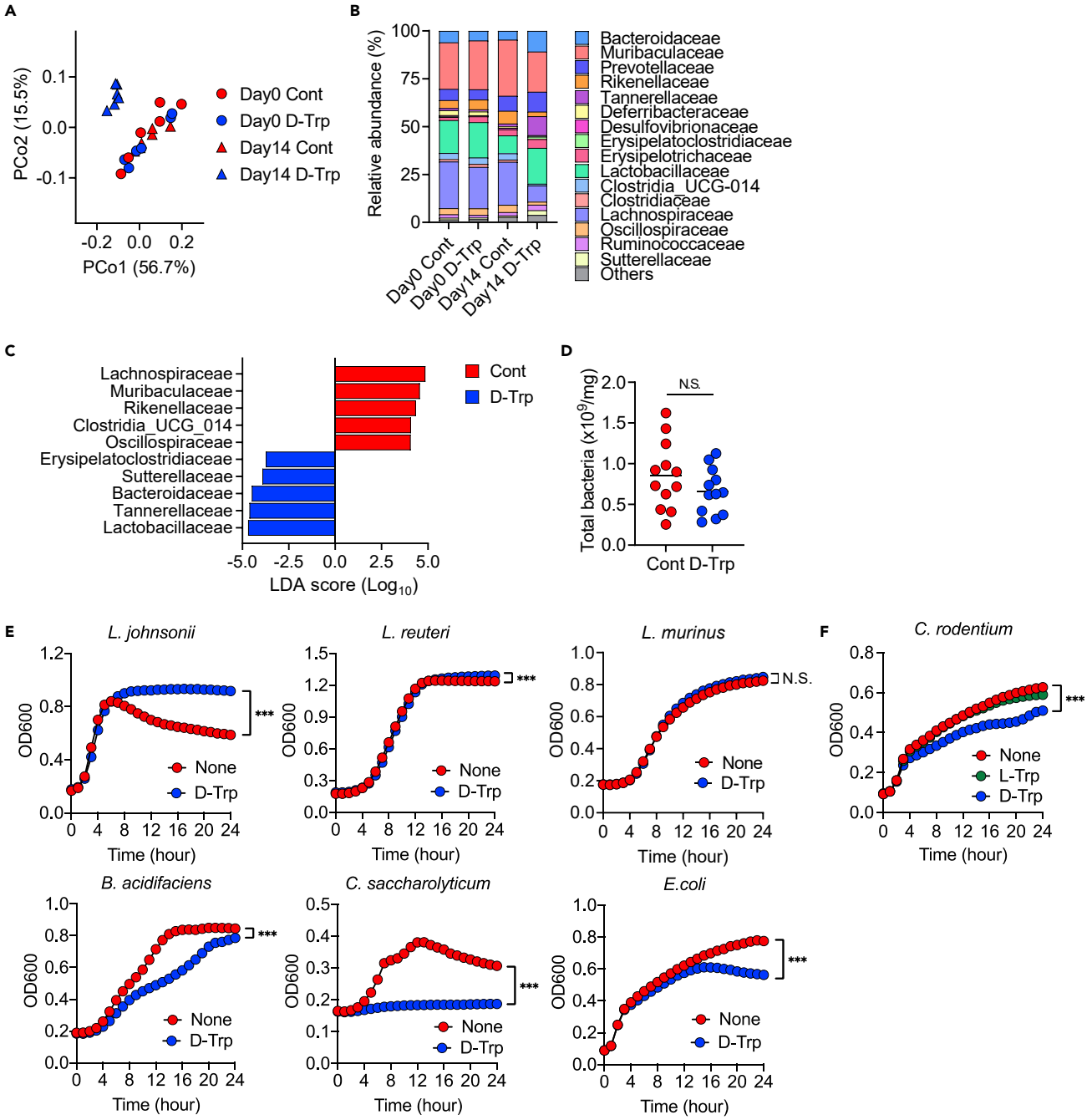

Figure 3. Effect of $_{D}$-Tryptophan on the composition of gut microbiota

(A-D) Specific pathogen-free (SPF) wild-type mice were fed with respective diets (Cont, unsupplemented diet; $_{D}$-Trp, 5% $_{D}$-Tryptophan supplemented diet) for 2 weeks, after which fecal samples were obtained to analyze the composition of the gut microbiota (A-C, n = 6; D, n = 12 mice per group).

(A) Principal coordinate analysis (PCA) plot generated using weighted UniFrac metric.

(B) Relative abundance of operational taxonomic units (OTUs) in fecal samples. Various colors correspond to each indicated bacterial family.

(C) Histogram of the linear discriminant analysis (LDA) scores computed for differentially abundant bacterial taxa in fecal samples.

(D) The total number of bacteria per milligram of the fecal samples.

(E) Optical density (OD) of individual bacterial species cultured in a medium supplemented with or without 20 mM$_{D}$-Tryptophan ($_{D}$-Trp) measured over time at 600 nm (n = 8 samples per group).

Figure 3. *Continued*

(F) OD of *Citrobacter rodentium* cultured in a medium supplemented with or without 20 mM $_D$-Tryptophan ($_D$-Trp) or $_L$-Tryptophan ($_L$-Trp) measured over time at 600 nm (n = 8 samples per group). Each dot represents one sample or mouse, or the mean ± SD. Horizontal bars indicate mean values. Statistical significance was assessed using unpaired Student's *t*-test in panel D, and two-way ANOVA with Šidák corrections for multiple comparisons in panels E and F. The asterisks in E and F indicate significant differences after 24 h. ***$p < 0.001$; N.S., not significant. All the experiments were conducted at least three independent times.

acidifaciens (whose abundance was increased by $_D$-Trp treatment), *Clostridium saccharolyticum*, belonging to Lachnospiraceae (whose abundance was decreased by $_D$-Trp treatment), *C. rodentium*, and *E. coli* were cultured in the absence and presence of $_D$-Trp. Consistent with the *in vivo* results, the growth of *Lactobacillus johnsonii* (*L. johnsonii*), *Limosilactobacillus reuteri* (*L. reuteri*), and *Ligilactobacillus murinus* (*L. murinus*) was promoted or remained unaffected by treatment with $_D$-Trp. The growth rate of *B. acidifaciens* was reduced by $_D$-Trp; however, the growth of the bacteria, eventually, increased and reached a level similar to that observed when cultured without $_D$-Trp (Figure 3E). By contrast, the proliferation of *C. saccharolyticum* was significantly inhibited in the presence of $_D$-Trp (Figure 3E). Furthermore, the growth of *C. rodentium* was also inhibited by $_D$-Trp but not by $_L$-Trp (Figure 3F). Collectively, these results indicate that $_D$-Trp directly and differentially influences the growth of each gut microbe.

$_D$-Tryptophan increases intracellular indole acrylic acid (IA), which determines the susceptibility of gut microbes to $_D$-Trp

To elucidate the mechanism by which $_D$-Trp influences the metabolism of the gut microbes, we performed unbiased capillary electrophoresis time-of-flight mass spectrometry (CE-TOFMS)-based metabolome analysis of the intracellular contents including tryptophan metabolites (Figure 4A) derived from the intestinal bacteria grown in the presence or absence of $_L$-Trp or $_D$-Trp. The volcano plot showed that the levels of several metabolites of *C. rodentium* were increased upon the addition of $_L$-Trp or $_D$-Trp (Figure 4B). Notably, the treatment of *C. rodentium* with $_D$-Trp increased the intracellular levels of tryptophan and its derivatives, particularly IA, hydroxy indole pyruvate, hydroxytryptophan, formyl kynurenine, and kynurenine (Figure 4C). Among the tryptophan derivatives, IA level was the highest in the *C. rodentium* treated with $_D$-Trp (Figures 4Band 4C), while the levels of other tryptophan derivatives, such as indole lactic acid and indole acetic acid, were higher in *C. rodentium* treated with $_L$-Trp than in untreated *C. rodentium* or those treated with $_D$-Trp (Figure 4C). Similarly, the intracellular level of IA was robustly increased in $_D$-Trp-treated *E. coli* but not in $_L$-Trp-treated or untreated *E. coli* (Figure 4D). In contrast, the intracellular level of IA was increased in $_L$-Trp-treated *Lactobacillus* species, including *L. johnsonii* and *L. reuteri*, which was comparable to the levels observed in $_D$-Trp-treated groups (Figure 4D). These results indicate that the level of IA was increased in $_D$-Trp-susceptible bacteria only in the presence of $_D$-Trp. However, $_D$-Trp-resistant bacteria accumulated IA in the presence of $_D$-Trp as well as $_L$-Trp. As $_D$-Trp-susceptible bacteria only generate IA upon $_D$-Trp treatment, we hypothesized that IA is the critical factor that is involved in the inhibition of the growth of gut microbes mediated by $_D$-Trp. As expected, treatment with IA significantly suppressed the growth of $_D$-Trp-susceptible *C. rodentium* and *E. coli*, but not $_D$-Trp-resistant *L. johnsonii* and *L. reuteri* (Figure 4E). To confirm the suppression of the growth of $_D$-Trp susceptible bacteria by IA *in vivo*, mice treated with IA were infected with *C. rodentium* and examined for bacterial burden and survival. Treatment with IA significantly prevented weight loss and improved survival in the mice infected with *C. rodentium* (Figures 4F and 4G). Moreover, the levels of fecal shedding of *C. rodentium* were comparable in both groups on days 3 and 6 post-infection but were significantly decreased in the mice treated with IA 9 days after the infection (Figure 4H). IA is known to act as an AhR ligand and enhances intestinal epithelial barrier function (Wlodarska et al., 2017). Indeed, treatment with IA enhanced the expression of *Cyp1a1* but not *Reg3g*, *Muc2*, and *Il10* (Figures S7A-S7D). In addition, fecal concentrations of lipocalin-2 were comparable between *C. rodentium*-infected mice given IA or not (Figure S7E). Although food intake was decreased for a couple of days and body weight was lower in the mice treated with 2.5% IA compared with the control group, the food consumption, eventually, became equal between the two groups, and treatment with IA did not cause mortality (Figure S8). These results suggest that IA, a tryptophan derivative, is a key factor associated with the susceptibility of gut microbes to $_D$-Trp, and treatment with IA inhibits the growth of $_D$-Trp-susceptible enteric pathogens.

DISCUSSION

Gut microbiota, such as Firmicutes which is the most relevant phylum, produce at least 12 free $_D$-AAs including $_D$-Trp (Matsumoto et al., 2018). In addition, certain lactic acid bacteria, such as *Bifidobacterium*

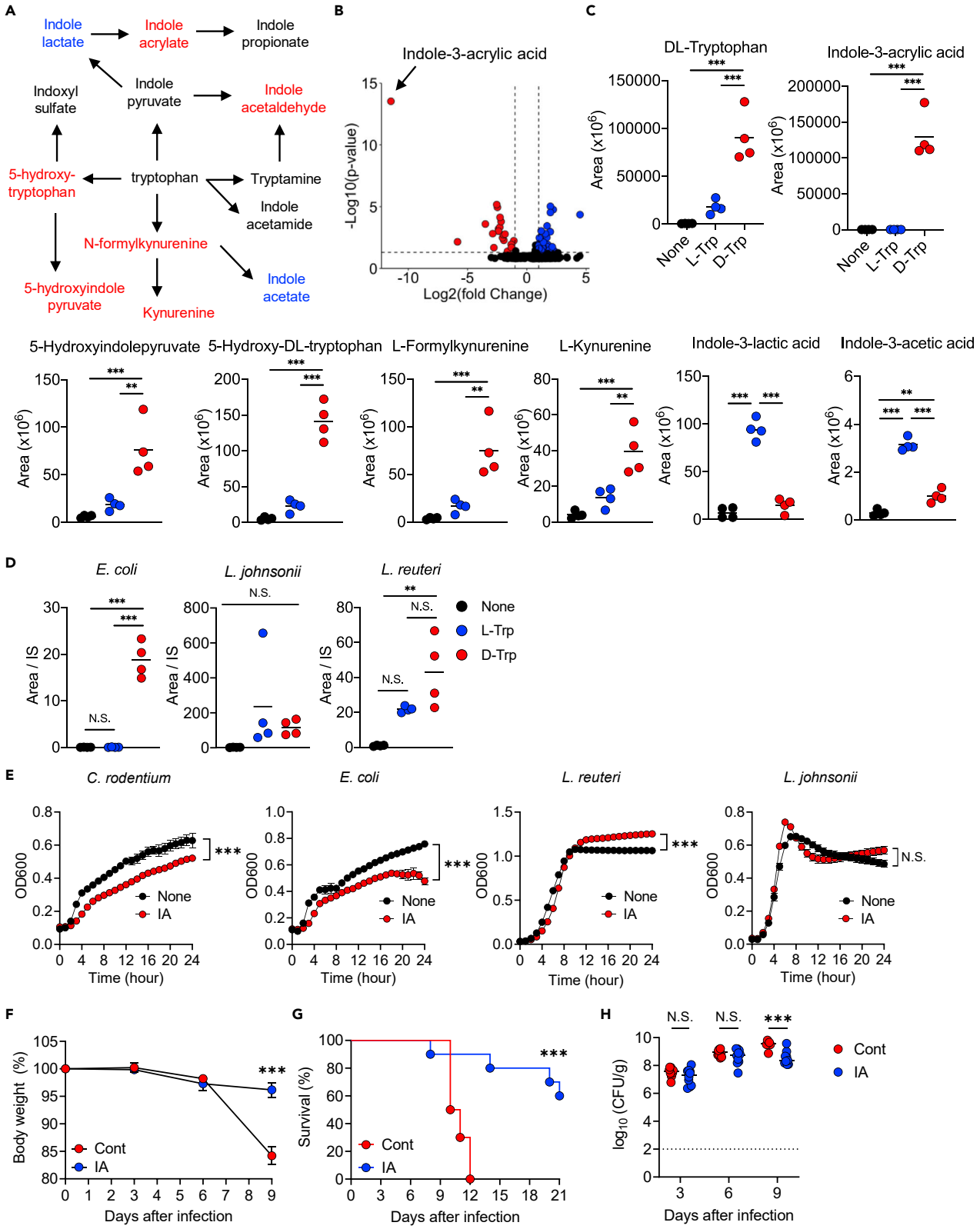
A
Indole lactate
Indole acrylate
Indole propionate
Indoxyl sulfate
Indole pyruvate
Indole acetaldehyde
5-hydroxy-tryptophan
tryptophan
Tryptamine
Indole acetamide
N-formylkynurenine
5-hydroxyindole pyruvate
Kynurenine
Indole acetate
B
Indole-3-acrylic acid
-Log10(p-value)
Log2(fold Change)
C
DL-Tryptophan
Indole-3-acrylic acid
Area (x10^6)
None
L-Trp
D-Trp
5-Hydroxyindolepyruvate
5-Hydroxy-DL-tryptophan
L-Formylkynurenine
L-Kynurenine
Indole-3-lactic acid
Indole-3-acetic acid
D
E. coli
L. johnsonii
L. reuteri
Area / IS
N.S.
None
L-Trp
D-Trp
E
C. rodentium
E. coli
L. reuteri
L. johnsonii
OD600
Time (hour)
None
IA
F
Body weight (%)
Cont
IA
Days after infection
G
Survival (%)
Cont
IA
Days after infection
H
log10 (CFU/g)
N.S.
N.S.
Cont
IA
Days after infection

Figure 4. Production of indoleacrylic acid (IA) by $_D$-Tryptophan in bacteria and its protective effect against enteric pathogens

(A-D) Metabolomic analysis of intracellular contents from the *Citrobacter rodentium* cultured in the presence or absence of 50 mM $_L$-Tryptophan ($_L$-Trp) or $_D$-Tryptophan ($_D$-Trp) for 24 h (n = 4 samples per group).

(A) Pathway of tryptophan metabolism. Colored dots represent significantly increased metabolite levels compared to None. Red: $_D$-Trp, Blue: $_L$-Trp.

(B) Volcano plot showing the significance and magnitude of differences in the relative abundance of intracellular metabolites grown in the presence of 50 mM $_L$-Trp or $_D$-Trp.

(C) The relative abundance of intracellular tryptophan and tryptophan derivatives.

(D) The relative abundance of intracellular indole-3-acrylic acid (IA) in *Escherichia coli*, *Lactobacillus johnsonii*, and *Limosilactobacillus reuteri* grown in the presence or absence of 50 mM $_L$-Trp or $_D$-Trp. IS; internal standard.

(E) Optical density (OD) of *E. coli*, *L. reuteri*, *L. johnsonii*, and *C. rodentium* grown in a medium supplemented with or without 2 mM IA measured over time at 600 nm (n = 8 samples per group).

(F-H) Mice were fed with respective diets (Cont, unsupplemented diet; IA, 2.5% IA supplemented diet) and then infected orally with 2×10^9 colony-forming units (CFU) of *C. rodentium* (n = 10 mice per group).

(F) Changes in body weight, (G) survival rate, and (H) fecal *C. rodentium* load on days 3, 6, and 9 post-infection. Each dot represents one sample or mouse, or the mean ± SD (E) or SEM (F). Horizontal bars indicate mean values. Statistical significance was assessed using Tukey's multiple comparison test in panels C and D, two-way ANOVA with Šidák corrections for multiple comparisons in panels E and F, Log-rank test in panels G, and unpaired Student's *t*-test in panel H, Asterisks in (E) indicate significant differences observed after 24 h. *$p < 0.05$; **$p < 0.01$; ***$p < 0.001$; N.S., not significant. All the experiments were conducted at least three independent times.

and *Lactobacillus*, produce and secrete $_D$-Trp (Kepert et al., 2017). However, the mechanism underlying the effect of $_D$-Trp on the gut environment is largely unknown. In this study, we found that $_D$-Trp inhibited the growth of enteric pathogen and colitogenic pathobionts and suppressed microbe-induced colitis. Although $_D$-Met showed the highest inhibition of the growth of *C. rodentium in vitro*, it offered only modest protection against lethal infection with *C. rodentium in vivo*. Most of the $_D$-Met is converted into the $_L$-Met (Hasegawa et al., 2005) in two steps. The initial step involves oxidative deamination by DAO to generate α-keto-γ-methiolbutyric acid, followed by stereo-specific re-amination into $_L$-Met by transaminases (Kaji et al., 1980; London and Gabel, 1988). Therefore, the administered $_D$-Met might be converted into $_L$-Met by mice enzymes. Indeed, fecal and plasma levels of $_D$-Met were lower than those of $_D$-Trp when the mice were administered with the same amounts of $_D$-AAs.

Treatment with $_D$-Trp strongly suppressed DSS- and T cell transfer-induced colitis. Furthermore, on treatment with DSS, the GF mice colonized with the gut microbiota from $_D$-Trp-treated mice showed lower loss of body weight than the GF mice colonized with the gut microbiota derived from untreated mice. These results indicate that $_D$-Trp directly acts on gut microbiota and reduces colitogenic bacteria. However, $_D$-Trp may influence host enzymes and immune cells and regulate gut inflammation. $_D$-AAs are enantiomers that are selectively recognized by host receptors and enzymes, including DAO, in mammals. In the gut mucosal tissue, where the host and microbes interface, DAO catalyzes the oxidation of bacterial $_D$-AAs and generates H_2O_2, which promotes pathogen elimination (Sasabe et al., 2016). $_D$-Trp also acts as a chemo-attractant for human leukocytes via G-protein-coupled receptor 109B (Irukayama-Tomobe et al., 2009), which may promote pathogen killing. Furthermore, $_D$-Trp produced by probiotic bacteria reduces the secretion of chemokine ligand 17 (CCL17) in T-cells. It increases IL-10 and decreases IFN-γ, IL-12, and IL-5 in human monocyte-derived dendritic cells when stimulated by LPS. In addition, oral treatment of mice with $_D$-Trp increases the number of regulatory T cells in the lung and the colon, decreases the lung Th2 response, and reduces allergic airway inflammation (Kepert et al., 2017). Therefore, $_D$-Trp could create an anti-inflammatory and anti-pathogenic environment by influencing the function of the immune cells.

$_L$-Trp metabolism, mediated by both host and gut microbiota, is a key modulator of the gut microbiome, which has a major impact on the physiological and pathological pathways. $_L$-Trp is metabolized by the host indoleamine 2,3-dioxygenase into Kynurenine, which exerts suppressive effects on inflammation and immune responses (Takamatsu et al., 2013). The gut microbiota also metabolizes $_L$-Trp into indole derivatives. Several of these indole derivatives, such as indole-3-aldehyde, indole-3-acid-acetic, indole-3-propionic acid, and indole-3-acetaldehyde, are activators of the AhR that promotes IL-22 production, which, in turn, stimulates mucosal defense via the production of antimicrobial proteins (Agus et al., 2018; Wang et al., 2014; Zelante et al., 2013). *Peptostreptococcus* species, such as *P. russellii*, a member of the gut microbiota, metabolizes tryptophan into IA, which enhances intestinal epithelial barrier function and reduces inflammatory responses (Wlodarska et al., 2017). IA also induces the expression of the AhR target gene *Cyp1a1*, suggesting that IA can act as an AhR ligand (Wlodarska et al., 2017). We observed that treatment with $_D$-Trp and IA as well as $_L$-Trp robustly enhanced the expression of *Cyp1a1*, suggesting that AhR

ligands, including IA, were produced or provided in the intestine of mice in these groups. However, D-Trp and IA but not L-Trp protected the mice from lethal infection with *C. rodentium*. Thus, the activation of AhR by D-Trp, L-Trp, or IA might not contribute to the prevention of colonic inflammation and diarrhea induced by *C. rodentium*. But it is still possible that D-Trp and IA directly act on the host AhR to contribute suppression of colitis. The experiments using AhR-deficient mice will reveal the role of AhR on the protective effects of D-Trp and IA.

IA was the key tryptophan derivative associated with the susceptibility of gut microbes including pathogens and colitogenic pathobionts to D-Trp. IA inhibits the conversion of indole to tryptophan mediated by tryptophan synthase, resulting in a depletion of the tryptophan pool and growth inhibition (Miozzari et al., 1977). IA also decreases the cellular levels of charged $tRNA^{Trp}$ (Bertrand and Yanofsky, 1976). Thus, treatment with D-Trp may influence tryptophan biosynthesis and protein synthesis in susceptible gut microbes via the generation of IA. Under normal conditions, not a large amount of D-Trp normally exists in the gut (Matsumoto et al., 2018). Thus, when the excess D-Trp is provided, certain bacteria may not handle their metabolism and D-Trp essentially acts as a xenobiotic to inhibit bacterial growth.

Our findings regarding the effect of D-Trp on enteric pathogens and colitogenic pathobionts demonstrate a novel biological function of D-Trp that can create a "healthy gut environment" to prevent colonic inflammation. Our results suggest that D-Trp itself, or strategies that increase the abundance of specific bacteria which produce D-Trp, could be used to control enteric pathogen infection and inflammatory bowel diseases. Given that D-Trp exerts an inhibitory effect on the growth of enteric pathogens and pathobionts, our findings provide further evidence of the contribution of D-AAs in the control of physiological functions in the host.

Limitations of the study and prospects

Here, we demonstrated the potential role of D-Trp in preventing or eliminating infections and colitis via control of gut microbiota and pathogens; however, our study has some limitations. First, D-Trp specifically increased the levels of IA in the D-Trp susceptible gut microbes, which inhibited their growth; However, why D-Trp was preferentially metabolized into IA in these microbes is largely unknown. Thus, we need to verify how IA is produced from D-Trp by using stable isotopes. Second, although we found oral supplementation with D-Trp inhibited the proliferation of pathogens and certain microbial species in the mice gut, thereby preventing colitis, physiological effects of D-Trp produced by gut bacteria on the host were not examined in this study. Therefore, it will be interesting to assess the importance of gut microbiota-derived D-Trp in the preventive and therapeutic effects of colitis. Future studies will include the identification of high D-Trp-producing gut microbes and verification of the protective function of bacteria-derived D-Trp against pathogens and pathobionts-induced colitis. Third, we could not identify how IA inhibits the growth of enteric pathogens and pathobionts. The experiments including transposon mutagenesis screening will identify the related genes and the mechanistic insights of bacterial growth inhibition by IA. Finally, translation from mice to humans of the findings, that D-Trp prevents colitis by suppressing the growth of pathogens and pathobionts, will be the most attractive future study.

STAR★METHODS

Detailed methods are provided in the online version of this paper and include the following:

- KEY RESOURCES TABLE
- RESOURCE AVAILABILITY
  - Lead contact
  - Materials availability
  - Data and code availability
- EXPERIMENTAL MODEL AND SUBJECT DETAILS
  - Mice
  - *C. rodentium* infection
  - Dextran sodium sulfate (DSS)-induced colitis
  - DSS-induced colitis in gut microbiota transferred-germ-free mice
  - T Cell transfer model of colitis

SUPPLEMENTAL INFORMATION

Supplemental information can be found online at https://doi.org/10.1016/j.isci.2022.104838.

ACKNOWLEDGMENTS

This work was supported by research grants from the JSPS KAKENHI (JP17H05068 and JP20H03490 to Y.-G.K.), AMED (JP18gm6010004h0003 to Y.-G.K.), Takeda Science Foundation (to Y.-G.K.), the Naito Foundation (to Y.-G.K.), Yakult Bio-Science Foundation (to Y.-G.K.), and Mochida Memorial Foundation for Medical and Pharmaceutical Research (to Y.-G.K.).

AUTHOR CONTRIBUTIONS

Y.-G.K. conceived the study and designed the experiments; N. S., T. K., M. G., G. Y., Y. S., K. Y., J. U., M. A., S. H., and Y.-G.K. collected samples and conducted the experiments; N. S., T. K., M. G., G. Y., Y. S., K. Y., J. U., M. A., S. H., T. H., M. S., K. H., and Y.-G. K. analyzed data; N. S., G.Y., M. A., and Y.-G. K. prepared the article. Y.-G. K. supervised the project. All authors read and approved the final article.

DECLARATION OF INTERESTS

This study was funded by Meiji Holdings Co. S.H. is an employee of Co-Creation Center, Meiji Holdings Co., Ltd. The other authors declare no competing interests.

Received: December 15, 2021
Revised: May 17, 2022
Accepted: July 21, 2022
Published: August 19, 2022

REFERENCES

Agus, A., Planchais, J., and Sokol, H. (2018). Gut microbiota regulation of tryptophan metabolism in health and disease. Cell Host Microbe *23*, 716–724. https://doi.org/10.1016/j.chom.2018.05.003.

Alvarez, L., Aliashkevich, A., de Pedro, M.A., and Cava, F. (2018). Bacterial secretion of D-arginine controls environmental microbial biodiversity. ISME J. *12*, 438–450. https://doi.org/10.1038/ismej.2017.176.

Barman, M., Unold, D., Shifley, K., Amir, E., Hung, K., Bos, N., and Salzman, N. (2008). Enteric salmonellosis disrupts the microbial ecology of the murine gastrointestinal tract. Infect. Immun. *76*, 907–915. https://doi.org/10.1128/IAI.01432-07.

Bertrand, K., and Yanofsky, C. (1976). Regulation of transcription termination in the leader region of the tryptophan operon of Escherichia coli involves tryptophan or its metabolic product. J. Mol. Biol. *103*, 339–349. https://doi.org/10.1016/0022-2836(76)90316-8.

Bolyen, E., Rideout, J.R., Dillon, M.R., Bokulich, N.A., Abnet, C.C., Al-Ghalith, G.A., Alexander, H., Alm, E.J., Arumugam, M., Asnicar, F., et al. (2019). Reproducible, interactive, scalable and extensible microbiome data science using QIIME 2. Nat. Biotechnol. *37*, 852–857. https://doi.org/10.1038/s41587-019-0209-9.

Borenshtein, D., McBee, M.E., and Schauer, D.B. (2008). Utility of the Citrobacter rodentium infection model in laboratory mice. Curr. Opin. Gastroenterol. *24*, 32–37. https://doi.org/10.1097/MOG.0b013e3282f2b0fb.

Callahan, B.J., McMurdie, P.J., Rosen, M.J., Han, A.W., Johnson, A.J.A., and Holmes, S.P. (2016). DADA2: high-resolution sample inference from Illumina amplicon data. Nat. Methods *13*, 581–583. https://doi.org/10.1038/nmeth.3869.

Camacho, C., Coulouris, G., Avagyan, V., Ma, N., Papadopoulos, J., Bealer, K., and Madden, T.L. (2009). BLAST+: architecture and applications. BMC Bioinf. *10*, 421. https://doi.org/10.1186/1471-2105-10-421.

Cava, F., Lam, H., de Pedro, M.A., and Waldor, M.K. (2011). Emerging knowledge of regulatory roles of D-amino acids in bacteria. Cell. Mol. Life Sci. *68*, 817–831. https://doi.org/10.1007/s00018-010-0571-8.

Chassaing, B., Srinivasan, G., Delgado, M.A., Young, A.N., Gewirtz, A.T., and Vijay-Kumar, M. (2012). Fecal lipocalin 2, a sensitive and broadly dynamic non-invasive biomarker for intestinal inflammation. PLoS One *7*, e44328. https://doi.org/10.1371/journal.pone.0044328.

Chen, G.Y., Shaw, M.H., Redondo, G., and Núñez, G. (2008). The innate immune receptor Nod1 protects the intestine from inflammation-induced tumorigenesis. Cancer Res. *68*, 10060–10067. https://doi.org/10.1158/0008-5472.CAN-08-2061.

D'Aniello, A. (2007). D-Aspartic acid: an endogenous amino acid with an important neuroendocrine role. Brain Res. Rev. *53*, 215–234. https://doi.org/10.1016/j.brainresrev.2006.08.005.

Devkota, S., Wang, Y., Musch, M.W., Leone, V., Fehlner-Peach, H., Nadimpalli, A., Antonopoulos, D.A., Jabri, B., and Chang, E.B. (2012). Dietary-fat-induced taurocholic acid promotes pathobiont expansion and colitis in Il10-/- mice. Nature *487*, 104–108. https://doi.org/10.1038/nature11225.

Dianda, L., Hanby, A.M., Wright, N.A., Sebesteny, A., Hayday, A.C., and Owen, M.J. (1997). T cell receptor-alpha beta-deficient mice fail to develop colitis in the absence of a microbial environment. Am. J. Pathol. *150*, 91–97.

Feng, T., Wang, L., Schoeb, T.R., Elson, C.O., and Cong, Y. (2010). Microbiota innate stimulation is a prerequisite for T cell spontaneous proliferation and induction of experimental colitis. J. Exp. Med. *207*, 1321–1332. https://doi.org/10.1084/jem.20092253.

Garrett, W.S., Lord, G.M., Punit, S., Lugo-Villarino, G., Mazmanian, S.K., Ito, S., Glickman, J.N., and Glimcher, L.H. (2007). Communicable ulcerative colitis induced by T-bet deficiency in the innate immune system. Cell *131*, 33–45. https://doi.org/10.1016/j.cell.2007.08.017.

Goodyear, A.W., Kumar, A., Dow, S., and Ryan, E.P. (2014). Optimization of murine small intestine leukocyte isolation for global immune phenotype analysis. J. Immunol. Methods *405*, 97–108. https://doi.org/10.1016/j.jim.2014.01.014.

Hancock, R. (1960). The amino acid composition of the protein and cell wall of Staphylococcus aureus. Biochim. Biophys. Acta *37*, 42–46. https://doi.org/10.1016/0006-3002(60)90076-7.

Harris, N.R., Whatley, J.R., Carter, P.R., Morgan, G.A., and Grisham, M.B. (2009). Altered microvascular hemodynamics during the induction and perpetuation of chronic gut inflammation. Am. J. Physiol. Gastrointest. Liver Physiol. *296*, G750–G754. https://doi.org/10.1152/ajpgi.90702.2008.

Hasegawa, H., Shinohara, Y., Akahane, K., and Hashimoto, T. (2005). Direct detection and evaluation of conversion of D-methionine into L-methionine in rats by stable isotope methodology. J. Nutr. *135*, 2001–2005. https://doi.org/10.1093/jn/135.8.2001.

Hashimoto, A., Nishikawa, T., Oka, T., Takahashi, K., and Hayashi, T. (1992). Determination of free amino acid enantiomers in rat brain and serum by high-performance liquid chromatography after derivatization with N-tert.-butyloxycarbonyl-L-cysteine and o-phthaldialdehyde. J. Chromatogr. *582*, 41–48. https://doi.org/10.1016/0378-4347(92)80300-f.

Hernandez-Chirlaque, C., Aranda, C.J., Ocon, B., Capitan-Canadas, F., Ortega-Gonzalez, M., Carrero, J.J., Suarez, M.D., Zarzuelo, A., Sanchez de Medina, F., and Martinez-Augustin, O. (2016). Germ-free and antibiotic-treated mice are highly susceptible to epithelial injury in DSS colitis. J. Crohns Colitis *10*, 1324–1335. https://doi.org/10.1093/ecco-jcc/jjw096.

Homma, H. (2007). Biochemistry of D-aspartate in mammalian cells. Amino Acids *32*, 3–11. https://doi.org/10.1007/s00726-006-0354-6.

Honda, K., and Littman, D.R. (2012). The microbiome in infectious disease and inflammation. Annu. Rev. Immunol. *30*, 759–795. https://doi.org/10.1146/annurev-immunol-020711-074937.

Hu, S., Wang, J., Ji, E.H., Christison, T., Lopez, L., and Huang, Y. (2015). Targeted metabolomic analysis of head and neck cancer cells using high performance ion chromatography coupled with a Q exactive HF mass spectrometer. Anal. Chem. *87*, 6371–6379. https://doi.org/10.1021/acs.analchem.5b01350.

Irukayama-Tomobe, Y., Tanaka, H., Yokomizo, T., Hashidate-Yoshida, T., Yanagisawa, M., and Sakurai, T. (2009). Aromatic D-amino acids act as chemoattractant factors for human leukocytes through a G protein-coupled receptor, GPR109B. Proc. Natl. Acad. Sci. USA *106*, 3930–3934. https://doi.org/10.1073/pnas.0811844106.

Kaji, H., Saito, N., Murao, M., Ishimoto, M., Kondo, H., Gasa, S., and Saito, K. (1980). Gas chromatographic and gas chromatographic–mass spectrometric studies on alpha-keto-gamma-methylthiobutyric acid in urine following ingestion of optical isomers of methionine. J. Chromatogr. *221*, 145–148. https://doi.org/10.1016/s0378-4347(00)81016-6.

Kamada, N., Kim, Y.G., Sham, H.P., Vallance, B.A., Puente, J.L., Martens, E.C., and Núñez, G. (2012). Regulated virulence controls the ability of a pathogen to compete with the gut microbiota. Science *336*, 1325–1329. https://doi.org/10.1126/science.1222195.

Kepert, I., Fonseca, J., Müller, C., Milger, K., Hochwind, K., Kostric, M., Fedoseeva, M., Ohnmacht, C., Dehmel, S., Nathan, P., et al. (2017). D-tryptophan from probiotic bacteria influences the gut microbiome and allergic airway disease. J. Allergy Clin. Immunol. *139*, 1525–1535. https://doi.org/10.1016/j.jaci.2016.09.003.

Kim, Y.G., Sakamoto, K., Seo, S.U., Pickard, J.M., Gillilland, M.G., 3rd, Pudlo, N.A., Hoostal, M., Li, X., Wang, T.D., Feehley, T., et al. (2017). Neonatal acquisition of Clostridia species protects against colonization by bacterial pathogens. Science *356*, 315–319. https://doi.org/10.1126/science.aag2029.

Kiriyama, Y., and Nochi, H. (2016). D-amino acids in the nervous and endocrine systems. Scientifica (Cairo), 6494621. https://doi.org/10.1155/2016/6494621.

Kolodkin-Gal, I., Romero, D., Cao, S., Clardy, J., Kolter, R., and Losick, R. (2010). D-amino acids trigger biofilm disassembly. Science *328*, 627–629. https://doi.org/10.1126/science.1188628.

Lam, H., Oh, D.C., Cava, F., Takacs, C.N., Clardy, J., de Pedro, M.A., and Waldor, M.K. (2009). D-amino acids govern stationary phase cell wall remodeling in bacteria. Science *325*, 1552–1555. https://doi.org/10.1126/science.1178123.

London, R.E., and Gabel, S.A. (1988). A deuterium surface coil NMR study of the metabolism of D-methionine in the liver of the anesthetized rat. Biochemistry *27*, 7864–7869. https://doi.org/10.1021/bi00420a042.

Lupp, C., Robertson, M.L., Wickham, M.E., Sekirov, I., Champion, O.L., Gaynor, E.C., and Finlay, B.B. (2007). Host-mediated inflammation disrupts the intestinal microbiota and promotes the overgrowth of Enterobacteriaceae. Cell Host Microbe *2*, 204. https://doi.org/10.1016/j.chom.2007.08.002.

Matsuki, T., Watanabe, K., Fujimoto, J., Kado, Y., Takada, T., and Matsumoto, K. (2004). Quantitative PCR with 16S rRNA-gene-targeted species-specific primers for analysis of human intestinal bifidobacteria. Appl. Environ. Microbiol. *70*, 167–173.

Matsumoto, M., Kunisawa, A., Hattori, T., Kawana, S., Kitada, Y., Tamada, H., Kawano, S., Hayakawa, Y., Iida, J., and Fukusaki, E. (2018). Free D-amino acids produced by commensal bacteria in the colonic lumen. Sci. Rep. *8*, 17915. https://doi.org/10.1038/s41598-018-36244-z.

Miozzari, G., Niederberger, P., and Hütter, R. (1977). Action of tryptophan analogues in Saccharomyces cerevisiae. Arch. Microbiol. *115*, 307–316. https://doi.org/10.1007/BF00446457.

Mori, H., and Inoue, R. (2010). Serine racemase knockout mice. Chem. Biodivers. *7*, 1573–1578. https://doi.org/10.1002/cbdv.200900293.

Park, J.T., and Strominger, J.L. (1957). Mode of action of penicillin. Science *125*, 99–101. https://doi.org/10.1126/science.125.3238.99.

Pruesse, E., Quast, C., Knittel, K., Fuchs, B.M., Ludwig, W., Peplies, J., and Glöckner, F.O. (2007). SILVA: a comprehensive online resource for quality checked and aligned ribosomal RNA sequence data compatible with ARB. Nucleic Acids Res. *35*, 7188–7196. https://doi.org/10.1093/nar/gkm864.

Qiu, J., Heller, J.J., Guo, X., Chen, Z.m.E., Fish, K., Fu, Y.X., and Zhou, L. (2012). The aryl hydrocarbon receptor regulates gut immunity through modulation of innate lymphoid cells. Immunity *36*, 92–104. https://doi.org/10.1016/j.immuni.2011.11.011.

Reinoso Webb, C., den Bakker, H., Koboziev, I., Jones-Hall, Y., Rao Kottapalli, K., Ostanin, D., Furr, K.L., Mu, Q., Luo, X.M., and Grisham, M.B. (2018). Differential susceptibility to T cell-induced colitis in mice: role of the intestinal microbiota. Inflamm. Bowel Dis. *24*, 361–379. https://doi.org/10.1093/ibd/izx014.

Sasabe, J., Miyoshi, Y., Rakoff-Nahoum, S., Zhang, T., Mita, M., Davis, B.M., Hamase, K., and Waldor, M.K. (2016). Interplay between microbial d-amino acids and host d-amino acid oxidase modifies murine mucosal defence and gut microbiota. Nat. Microbiol. *1*, 16125. https://doi.org/10.1038/nmicrobiol.2016.125.

Sellon, R.K., Tonkonogy, S., Schultz, M., Dieleman, L.A., Grenther, W., Balish, E., Rennick, D.M., and Sartor, R.B. (1998). Resident enteric bacteria are necessary for development of

spontaneous colitis and immune system activation in interleukin-10-deficient mice. Infect. Immun. *66*, 5224–5231. https://doi.org/10.1128/IAI.66.11.5224-5231.1998.

Takamatsu, M., Hirata, A., Ohtaki, H., Hoshi, M., Hatano, Y., Tomita, H., Kuno, T., Saito, K., and Hara, A. (2013). Ido1 plays an immunosuppressive role in 2, 4, 6-trinitrobenzene sulfate-induced colitis in mice. J. Immunol. *191*, 3057–3064. https://doi.org/10.4049/jimmunol.1203306.

Taurog, J.D., Richardson, J.A., Croft, J.T., Simmons, W.A., Zhou, M., Fernández-Sueiro, J.L., Balish, E., and Hammer, R.E. (1994). The germfree state prevents development of gut and joint inflammatory disease in HLA-B27 transgenic rats. J. Exp. Med. *180*, 2359–2364. https://doi.org/10.1084/jem.180.6.2359.

te Velde, A.A., de Kort, F., Sterrenburg, E., Pronk, I., ten Kate, F.J.W., Hommes, D.W., and van Deventer, S.J.H. (2007). Comparative analysis of colonic gene expression of three experimental colitis models mimicking inflammatory bowel disease. Inflamm. Bowel Dis. *13*, 325–330. https://doi.org/10.1002/ibd.20079.

Wang, X., Ota, N., Manzanillo, P., Kates, L., Zavala-Solorio, J., Eidenschenk, C., Zhang, J., Lesch, J., Lee, W.P., Ross, J., et al. (2014). Interleukin-22 alleviates metabolic disorders and restores mucosal immunity in diabetes. Nature *514*, 237–241. https://doi.org/10.1038/nature13564.

Weiss, S., Xu, Z.Z., Peddada, S., Amir, A., Bittinger, K., Gonzalez, A., Lozupone, C., Zaneveld, J.R., Vázquez-Baeza, Y., Birmingham, A., et al. (2017). Normalization and microbial differential abundance strategies depend upon data characteristics. Microbiome *5*, 27. https://doi.org/10.1186/s40168-017-0237-y.

Wlodarska, M., Luo, C., Kolde, R., d'Hennezel, E., Annand, J.W., Heim, C.E., Krastel, P., Schmitt, E.K., Omar, A.S., Creasey, E.A., et al. (2017). Indoleacrylic acid produced by commensal peptostreptococcus species suppresses inflammation. Cell Host Microbe. *22*, 25–37.e6. https://doi.org/10.1016/j.chom.2017.06.007.

Zelante, T., Iannitti, R.G., Cunha, C., De Luca, A., Giovannini, G., Pieraccini, G., Zecchi, R., D'Angelo, C., Massi-Benedetti, C., Fallarino, F., et al. (2013). Tryptophan catabolites from microbiota engage aryl hydrocarbon receptor and balance mucosal reactivity via interleukin-22. Immunity *39*, 372–385. https://doi.org/10.1016/j.immuni.2013.08.003.

STAR★METHODS

KEY RESOURCES TABLE

REAGENT or RESOURCE	SOURCE	IDENTIFIER
Antibodies		
anti-mouse CD16/CD32 antibody (clone 93)	BioLegend	Cat#101320; RRID: AB_1574975
BV510 CD45 (clone 30-F11)	BioLegend	Cat#103138; RRID: AB_2563061
BV510 Ly6G (clone 1A8)	BD	Cat#740157; RRID: AB_2739910
Alexa Fluor 488 F4/80 (clone BM8)	BioLegend	Cat#123120; RRID: AB_893479
Phycoerythrin (PE) CD11b (clone M1/70)	Thermo Fisher Scientific	Cat#12-0112-83; RRID: AB_2734869
PE-CF594 Siglec-F (clone E50-2440)	BD	Cat#562757; RRID: AB_2687994
PE-Cy7 CD4 (clone GK1.5)	Thermo Fisher Scientific	Cat#25-0041-8; RRID: AB_469576
PE-Cy7 CD11c (clone HL3)	BD	Cat#558074; RRID: AB_1645213
Allophycocyanin (APC) Ly6C (clone AL-21)	BD	Cat#560595; RRID: AB_1727554
APC CD45R/B220 (clone RA3-6B2)	BioLegend	Cat#553092; RRID: AB_398531
APC-Cy7 TCRβ (clone H57-597)	BioLegend	Cat#109220; RRID: AB_893624
7-AAD Viability Staining	BioLegend	Cat#420404; RRID:
Fixable Viability Stain 780	BD	Cat#565388; RRID: AB_2869673
Bacterial and virus strains		
C. rodentium strain DBS120 (pCRP1:: Tn5)	Kim et al. (2017)	N/A
Chemicals, peptides, and recombinant proteins		
Kanamycin	Nacalai Tesque	Cat# 19860–44; CAS: 25389-94-0
Luria-Bertani (LB) broth	Nacalai Tesque	Cat# 20066-95
LB agar	Nacalai Tesque	Cat# 20067-85
D-PBS (−)	Nacalai Tesque	Cat# 14249-95
MacConkey agar	BD Bioscience	Cat# 281810
Dextran sodium sulfate (DSS)	MP Biomedicals	CAS: 9011-18-1 Cat# 160110
carboxymethyl cellulose (CMC)	Nacalai Tesque	Cat# 07326-95 CAS: 9004-32-4
D-tryptophan	TCI	Cat# T0539 CAS: 153-94-6
D-methionine	Nacalai Tesque	Cat# 21717-51 CAS: 348-67-4
D(+)-phenylalanine	Nacalai Tesque	Cat# 26908-01 CAS: 673-06-3
D-leucine	Wako	Cat# 120-03551 CAS: 328-38-1
D-α-alanine	Nacalai Tesque	Cat# 01113-84 CAS: 338-69-2
D(+)-threonine	Wako	Cat# 206-07661 CAS: 632-20-2
D-valine	Wako	Cat# 222-00801 CAS: 640-68-6
D-asparagine monohydrate	Wako	Cat# 012-18991 CAS: 5794-24-1

(*Continued on next page*)

Continued

REAGENT or RESOURCE	SOURCE	IDENTIFIER
D(-)-arginine	Nacalai Tesque	Cat# 03331-51 CAS: 157-06-2
D(-)-lysine monohydrochloride	Wako	Cat# 128-04951 CAS: 7274-88-6
D-histidine	Wako	Cat# 085-05673 CAS: 351-50-8
D-glutamic Acid	Nacalai Tesque	Cat# 16909-01 CAS: 6893-26-1
D(+)-proline	Nacalai Tesque	Cat# 28925-11 CAS: 344-25-2
D(-)-isoleucine	Wako	Cat# 090-04183 CAS: 319-78-8
D(+)-tyrosine	Wako	Cat# 203-04393 CAS: 556-02-5
D-cysteine hydrochloride monohydrate	Wako	Cat# 034-13811 CAS: 207121-46-8
D-glutamine	TCI	Cat# G0278 CAS: 5959-95-5
D-aspartic acid	Nacalai Tesque	Cat# 03501-34 CAS: 1783-96-6
D-serine	Nacalai Tesque	Cat# 30606-21 CAS: 312-84-5
L-tryptophan	TCI	Cat# T0541 CAS: 73-22-3
NaOH	Nacalai Tesque	Cat# 94611-45
Tris-HCl	Nacalai Tesque	Cat# 35435-11
Glycerol	Nacalai Tesque	Cat# 17017-35
MRS broth	BD Bioscience	Cat# 288130
Agar	STAR	Cat# RSV-AGRP-500G
GAM agar	Nissui	Cat# 05426
BHI agar	BD Bioscience	Cat# 211065
Acetonitrile	Wako	Cat# 012-19851
Ethanol	Nacalai Tesque	Cat# 08948-25 CAS: 64-17-5
Mildform® 10N	Wako Pure Chemical	Cat# 133-10311
Hematoxylin	Agilent Technologies	Cat# CS70030-2
Eosin	Wako Pure Chemical	Cat# 058-00062 CAS: 17372-87-1
EDTA	Nacalai Tesque	Cat# 14347-21
HBSS (-)	Nacalai Tesque	Cat# 17460-15
HEPES-KOH Buffer Solution (pH7.5)	Nacalai Tesque	Cat# 15639-84
RPMI1640	Nacalai Tesque	Cat# 30264-56
Liberase TM	Roche Diagnostics	Cat# 05401127001
DNase I	Merck	Cat# 69182-3CN
NBCS	Thermo Fisher Scientific	Cat# RO-26010074
Penicillin Streptomycin Mix	Nacalai Tesque	Cat# 09367-34
Streptomycin Sulfate	Nacalai Tesque	Cat# 32237-14

(*Continued on next page*)

Continued

REAGENT or RESOURCE	SOURCE	IDENTIFIER
Methionine sulfone	Wako	Cat# 502-76641
2-morpholinoethanesulfonic acid	Dojindo	Cat# 349-01623
Critical commercial assays		
$CD4^+$ T Cell Isolation Kit, mouse	Miltenyi Biotec	Cat# 130-104-454
CD25 MicroBead Kit, mouse	Miltenyi Biotec	Cat# 130-091-072
KOD FX Neo	TOYOBO	Cat# KFX-201
mouse Lipocalin-2/NGAL DuoSet ELISA	R&D Systems	Cat# DY1857-05
PureLink® RNA Mini Kit	Thermo Fisher Scientific	Cat# 12183018A
ReverTra Ace® qPCR RT Master Mix with gDNA Remover	TOYOBO	Cat# FSQ-301
THUNDERBIRD® SYBR® qPCR Mix	TOYOBO	Cat# QPS-201
E.Z.N.A.®Stool DNA Kit	OMEGA	Cat# D4015-02
NEBNext® Ultra™ RNA Library Prep Kit for Illumina	Illumina	Cat# E7530L
NEBNext® Multiplex Oligos for Illumina® (Index Primers Set 1&2)	Illumina	Cat# E7335L
KAPA HiFi HotStart ReadyMix	Nippon Genetics	Cat# KK2602
AMPure XP	Beckman Coulter	Cat# A63881
Nextera XT index kit	Illumina	Cat# FC-131-200
Miseq Reagent Kit V3 (600 Cycle)	Illumina	Cat# MS-102-3003
Experimental models: Organisms/strains		
Mouse: C3H/HeN *Mus musculus*	CLEA Japan	C3H/HeNJcl
Mouse: C57BL/6J *Mus musculus*	Sankyo Labo Service	C57BL/6JJmsSlc
Mouse: Germ-free C57BL/6NCr	Sankyo Labo Service	C57BL/6NCr
Oligonucleotides		
Primers for total 16S rRNA gene Forward: TCCTACGGGAGGCAGCAGT	This paper	N/A
Primers for total 16S rRNA gene Reverse: GGACTACCAGGGTATCTAATCCTGTT	This paper	N/A
Primers for 16S rRNA gene sequencing Forward: CCAAACTCCTACGGGAGGCAGCAG	This paper	N/A
Primers for 16S rRNA gene sequencing Reverse: CATGGACTACCAGGGTATCTAATC	This paper	N/A
Primers for the V3 to V4 region of the 16S rRNA gene sequencing Forward: TCGTCGGCAGCGTCAGATGTGTATAA GAGACAGCCTACGGGNGGCWGCAG	This paper	N/A
Primers for the V3 to V4 region of the 16S rRNA gene sequencing Reverse: GTCTCGTGGGCTCGGAGATGTGTATAAG AGACAGGACTACHVGGGTATCTAATCC	This paper	N/A
Primers for mouse *Tbp* gene sequencing Forward: ACCGTGAATCTTGGCTGTAAA	This paper	N/A

(*Continued on next page*)

Continued

REAGENT or RESOURCE	SOURCE	IDENTIFIER
Primers for mouse *Tbp* gene sequencing Reverse: GCAGCAAATCGCTTGGGATTA	This paper	N/A
Primers for mouse *Tnf* gene sequencing Forward: CAGGCGGTGCCTATGTCTC	This paper	N/A
Primers for mouse *Tnf* gene sequencing Reverse: CGATCACCCCGAAGTTCAGTAG	This paper	N/A
Primers for mouse *Il1b* gene sequencing Forward: GAAATGCCACCTTTTGACAGTG	This paper	N/A
Primers for mouse *Il1b* gene sequencing Reverse: TGGATGCTCTCATCAGGACAG	This paper	N/A
Primers for mouse *Il6* gene sequencing Forward: TGATGCACTTGCAGAAAACA	This paper	N/A
Primers for mouse *Il6* gene sequencing Reverse: ACCAGAGGAAATTTTCAATAGGC	This paper	N/A
Primers for mouse *Reg3g* gene sequencing Forward: ATGCTTCCCCGTATAACCATCA	This paper	N/A
Primers for mouse *Reg3g* gene sequencing Reverse: ACTTCACCTTGCACCTGAGAA	This paper	N/A
Primers for mouse *Muc2* gene sequencing Forward: AGGGCTCGGAACTCCAGAAA	This paper	N/A
Primers for mouse *Muc2* gene sequencing Reverse: CCAGGGAATCGGTAGACATCG	This paper	N/A
Software and algorithms		
Qiime2 (version 2020.11)	QIIME 2 development team	Bolyen et al., 2019
GraphPad Prism software version 8.3.0 for Mac	GraphPad Software	https://www.graphpad.com/scientific-software/prism/
Waters TargetLynx™ software	Waters	https://www.waters.com/waters/ja_JP/TargetLynx-/nav.htm?cid=513791&locale=ja_JP
DADA2 algorithm	Benjamin Callahan	Callahan et al., 2016
BLAST	National Center for Biotechnology Information	Pruesse et al., 2007
SILVA database (version 138)	The SILVA ribosomal RNA database project	Camacho et al., 2009
Other		
SpectraMax iD3	Molecular Devices	https://www.moleculardevices.co.jp/systems/spectramax-id3-multi-mode-microplate-reader#gref
Miseq sequencer	Illumina	https://jp.illumina.com/systems/sequencing-platforms/miseq.html

(*Continued on next page*)

Continued

REAGENT or RESOURCE	SOURCE	IDENTIFIER
magLEAD 12gc	Precision system science	https://www.pss.co.jp/product/magtration/lead6-12gc.html
TQD	Waters	https://materials.waters.com/xevo-tqd-ms/
Quattro premier XE	Waters	https://www.waters.com/webassets/cms/library/docs/720001251en.pdf
CROWNPAK CR-I (+) column (3.0 mm i.d. × 150 mm, 5 μm particles)	Daicel	https://www.daicelchiral.com/products/crownpak-cr-i/
Mount-Quick	Daido Sangyo	http://www.daido-sangyo.co.jp/en/en_product/en_medical/en_mq_a.html
StepOnePlus	Thermo Fisher Scientific	https://www.thermofisher.com/order/catalog/product/4376598?SID=srch-srp-4376598
MACSQuant	Miltenyi Biotec	https://www.miltenyibiotec.com/JP-en/products/macs-flow-cytometry/flow-cytometers.html#gref
Ultrafree MC-PLHCC	Human Metabolome Technologies	https://humanmetabolome.com/jpn/service/goods/
SpeedVac	Thermo Fisher Scientific	https://www.thermofisher.com/order/catalog/product/DNA130-230?SID=srch-srp-DNA130-230
Q-Exactive focus	Thermo Fisher Scientific	https://www.thermofisher.com/jp/ja/home/industrial/mass-spectrometry/liquid-chromatography-mass-spectrometry-lc-ms/lc-ms-systems/orbitrap-lc-ms/q-exactive-orbitrap-mass-spectrometers.html
ICS-5000+	Thermo Fisher Scientific	https://www.thermofisher.com/order/catalog/product/22171-60002?SID=srch-srp-22171-60002
Dionex AERS 500	Thermo Fisher Scientific	https://www.thermofisher.com/order/catalog/product/085028?SID=srch-srp-085028
Thermo Scientific Dionex IonPac AS11-HC	Thermo Fisher Scientific	https://www.thermofisher.com/order/catalog/product/052961?SID=srch-srp-052961

RESOURCE AVAILABILITY

Lead contact

Further information and requests for resources and reagents should be directed to, and will be fulfilled by, the lead contact, Yun-Gi Kim (ykim@keio.jp).

Materials availability

This study did not generate new unique reagents.

Data and code availability

All data reported in this paper will be shared by the lead contact upon request.

This paper does not report original code.

Any additional information required to reanalyze the data reported in this paper is available from the lead contact upon request.

EXPERIMENTAL MODEL AND SUBJECT DETAILS

Mice

For infection experiments, 4-week-old female C3H/HeN mice were purchased from CLEA Japan Inc (Tokyo, Japan) and acclimated for 2 weeks. For colitis experiments, 6-week-old wild-type male C57BL/6J mice and germ-free male C57BL/6NCr mice were purchased from Sankyo Labo Service Corporation (Tokyo, Japan) and were acclimated for a week. All mice were housed at Keio University Faculty of Pharmacy, Tokyo. All experiments were approved by the ethics committees of Keio University.

C. rodentium infection

A kanamycin-resistant wild-type *C. rodentium* strain DBS120 (pCRP1:: Tn5) was used (Kim et al., 2017). For inoculations, bacteria were cultured overnight in Luria-Bertani (LB) broth supplemented with kanamycin (50 μg/mL) with shaking at 37°C. Mice were fed with a chow diet with or without 0.2%, 1%, or 5% of $_D$-Methionine or $_D$-Tryptophan or 2.5% 3-indoleacrylic acid from 10 days before the *C. rodentium* infection to the end of the experiment. These mice were infected with 0.2 mL of PBS containing approximately 1×10^9 CFU of *C. rodentium* administered via oral gavage. To determine the bacterial load in the feces or tissues, fecal pellets were collected from individual mice, homogenized in cold PBS, and plated at serial dilutions on MacConkey agar containing 50 μg/mL kanamycin. CFU was determined after overnight incubation at 37°C. The mice were euthanized 10 days after infection.

Dextran sodium sulfate (DSS)-induced colitis

Male 6-week-old mice were administered with 2% DSS (36–50 kDa; MP Biomedicals; Illkirch, France) in drinking water for 5 days for the induction of colitis, followed by 4–9 days of recovery with regular water. For pretreatment, mice were administered with 0.5% carboxymethyl cellulose (CMC) or 5% $_D$-Tryptophan ($_D$-Trp) (TCI; Tokyo, Japan) suspended in 0.5% CMC. A total of 1 mL of the CMC solution was administered per day with or without 5% $_D$-Trp via oral gavage from 2 weeks before the DSS administration to the end of the experiment. For therapeutic experiments, mice were given these from the end of the DSS treatment to the end of the experiment.

DSS-induced colitis in gut microbiota transferred-germ-free mice

Wild-type donor mice were orally administered with 0.5% CMC or 5% $_D$-Tryptophan suspended in 0.5% CMC (1 mL) per day for 2 weeks and then co-housed with germ-free C57BL/6NCr for 2 weeks. Mice were administered with 2% DSS supplemented in drinking water for 5 days for the induction of colitis, followed by 4–9 days of recovery with regular water. Donor mice were treated with CMC or $_D$-Trp suspended in CMC till the end of the experiment.

T Cell transfer model of colitis

Single-cell suspensions of splenocytes derived from wild-type female C57BL/6 donor mice were subjected to positive selection of $CD4^+$ T Cells via $CD4^+$ T Cell Isolation Kit, mouse (Miltenyi Biotec, Bergisch Gladbach, Germany). $CD25^+$ cells were depleted from $CD4^+$ T cell suspensions using the CD25 MicroBead Kit, mouse (Miltenyi Biotec). A total of 5×10^5 cells were transferred to each *Rag1*$^{-/-}$ mice recipient via intraperitoneal injection.

METHOD DETAILS

Pathogen growth with $_D$-amino acids and 3-indoleacrylic acid

Citrobacter rodentium were cultured on LB plates (Nacalai Tesque; Kyoto, Japan). Single colonies were inoculated into 10 mL LB broth aerobically and grown at 37 °C with shaking overnight. To examine growth dynamics, a 1:200 dilution of the overnight culture was inoculated. The LB medium was supplemented with each $_D$-amino acid and 3-indoleacrylic acid at a concentration of 50 mM and 2 mM, respectively. Incubation and optical density (OD) measurements were performed with SpectraMax iD3 (Molecular Devices, CA, USA) at 37 °C without shaking, and OD600 was measured at 1 h intervals for 24 h.

Isolation of intestinal resident bacteria and growth with $_D$-amino acids and 3-indoleacrylic acid

Lactobacillus johnsonii, *Limosilactobacillus reuteri*, *Ligilactobacillus murinus*, *Bacteroides acidifaciens*, *Clostridium saccharolyticum*, and *Escherichia coli* were isolated from the feces of mice. Every single colony

was resuspended in 50 mM NaOH, and boiled at 95 °C for 10 min. The sample was centrifuged at 3,000 rpm for 10 min, followed by the addition of 20 μL of the sample to 100 μL of Tris-HCl (pH 7.0–7.2). PCR was performed using KOD FX Neo (TOYOBO; Osaka, Japan) and the primer set specific to the 16S rRNA gene (Key Resources Table). The amplification was performed using primers with one cycle at 95 °C for 30 s, 30 cycles at 95 °C for 1 min followed by 60 °C for 45 s, ending the reaction at 72 °C for 35 s. Sanger sequencing was performed using Hokkaido System Science (Japan). The sequences were putatively identified corresponding to each bacterial strain using Microbial Nucleotide BLAST. Each isolate was stored in broth with 30% glycerol at −80 °C. For the growth experiment, *L. johnsonii*, *L. reuteri*, and *L. murinus* were cultured on MRS plates (BD Bioscience, CA, USA), and *E. coli* was cultured on LB plate (Nacalai Tesque) under aerobic conditions. *B. acidifaciens* was cultured on the GAM plate (Nissui, Tokyo, Japan), and *C. saccharolyticum* was cultured on the BHI plate (BD Bioscience) under anaerobic conditions.

Single colonies were inoculated into the corresponding broth and grown at 37 °C overnight. To analyze the growth dynamics, a 1:100 dilution of the overnight culture was inoculated. The medium was supplemented with 20 mM $_D$- or $_L$-Tryptophan or 2 mM 3-indoleacrylic acid. A non-supplemented medium was also used for the experiments. Incubation and OD measurements were performed with SpectraMax iD3 (Molecular Devices) at 37 °C without shaking, and OD600 was measured at 1 h intervals for 24 h.

Concentrations of $_D$-amino acids ($_D$-AAs)

Concentrations of serum and fecal $_D$-Tryptophan ($_D$-Trp) and $_D$-Methionine ($_D$-Met) were determined using LC-MS/MS system (Quatro premier XE, Waters Corporation). All analyses were performed using a CROWNPAK CR-I (+) column (3.0 mm i.d. × 150 mm, 5 μm particles) (Daicel Corporation, Osaka, Japan), which was used for the separation of $_D$- and $_L$-AAs. The mobile phase consisted of a mixture of 80% (v/v) acetonitrile, 15% (v/v) ethanol, 5% (v/v) Milli-Q water, and 0.4% (v/v) trifluoroacetic acid, and the flow rate was set to 0.35 mL/min under isocratic conditions. The injection volume was set at 2 μL, and the column temperature was set at 30 °C. The analytes were detected using electrospray ionization in the positive mode. Multiple reaction monitoring was performed using characteristic fragmentation ions m/z 205.1 > 132.0 for $_L$-Trp and $_D$-Trp and m/z 150.1 > 56.1 for $_L$-Met and $_D$-Met. The parameters for the LC-MS/MS analysis of $_D$/L-AAs were set as follows: capillary voltage, 3000 V; source temperature, 120 °C; desolvation temperature, 400 °C; desolvation gas flow, 850 L/h; cone gas flow, 50 L/h; cone voltage, 30 V; and collision energy, 10 eV. Mouse serum was mixed in the same volume of 5% TCA, and fecal samples were suspended in a 2-fold weight of 5% TCA. After mixing, the sample was centrifuged at 15,000 × g for 10 min at 4 °C. Then, 50 μL of the supernatant was transferred to a new 1.5 mL tube and mixed with 200 μL of mobile phase solution. The diluted sample was subjected to LC-MS/MS analysis. Data were analyzed using the Waters TargetLinks™ software.

Fecal Lipocalin-2

We measured the fecal lipocalin-2 level as a non-invasive intestinal inflammation biomarker (Chassaing et al., 2012). Mouse fecal pellets were collected in sterile 1.5 mL microcentrifuge tubes, and 100 mg/mL suspensions in sterile 0.1% Tween-20/D-PBS (−) were prepared. Samples were shaken using a vortex mixer at maximum speed for 20 min followed by centrifugation. The supernatants were assayed for lipocalin-2 using mouse Lipocalin-2/NGAL DuoSet ELISA (R&D Systems; MN, USA).

Histological analysis

Colonic tissue samples were fixed in 10% formalin neutral buffer solution (Mildform 10N, Wako Pure Chemical Industries, Osaka, Japan) overnight. After fixation, the samples were embedded in paraffin and then cut into 3 μm sections. The sections were deparaffinized, rehydrated, and stained with hematoxylin (Agilent Technologies, Inc., CA, USA) and eosin (Wako Pure Chemical Industries) and mounted using the aqueous mounting medium Mount-Quick (Daido Sangyo Co., Ltd., Saitama, Japan). Histologic evaluation was performed in a blinded fashion, using a scoring system described previously with some modifications (Chen et al., 2008). Briefly, a three- to four-point scale was used to denote the severity of inflammation (0, none; 1, mild; 2, moderate; and 3, severe), the level of involvement (0, none; 1, mucosa; 2, mucosa and submucosa; and 3, transmural), and extent of epithelial/crypt damage (0, none; 1, basal 1/3; 2, basal 2/3; 3, crypt loss; 4, crypt and surface epithelial destruction). Each variable was then multiplied by a factor reflecting the percentage of the cecum involved (0–25%, 26–50%, 51–75%, and 76–100%), and then summed to obtain the overall score.

Reverse transcription and quantitative PCR

Total RNA from mice tissue was extracted using the PureLink RNA Mini Kit (Thermo Fisher Scientific; MA, USA) according to the manufacturer's instructions. RNA was reverse-transcribed to obtain cDNA using the ReverTra Ace qPCR RT Master Mix with gDNA Remover (TOYOBO; Osaka, Japan). RT-qPCR was performed using the StepOnePlus (Thermo Fisher Scientific) with THUNDERBIRD SYBR qPCR Mix (TOYOBO). Oligonucleotide primers were purchased from Integrated DNA Technologies (Iowa, USA). Primer sequences are listed in Key resources table.

Determination of total 16S genes in feces

Mouse fecal pellets were collected in sterile 1.5 mL microcentrifuge tubes and resuspended in sterile D-PBS (−). DNA was extracted from 10-fold serial dilutions of the cultures and used as a standard for quantification of total bacteria in fecal samples. Bacterial DNA was isolated from fecal samples (or 200 μL of standard culture) using the method previously described by Matsuki et al. (2004). The 20-fold diluted fecal solution (200 μL) was mixed with 300 μL of extraction buffer (100 mM Tris–HCl, 40 mM EDTA, 1.7% SDS, pH 9.0), 500 μL of buffer-saturated phenol, and 300 mg of glass beads. The mixture was shaken at 500 × g for 5 min. After centrifugation at 15,000 × g for 5 min, 400 μL of the supernatant was collected. Subsequently, phenol-chloroform extractions were performed, and 250 μL of the supernatant was subjected to isopropanol precipitation. Finally, the DNA was suspended in 1 mL of TE (10 mM Tris–HCl, 1 mM EDTA, pH 8.0). The total number of bacteria in the feces was analyzed with quantitative real-time PCR using a universal primer. PCR amplification and detection were performed with StepOnePlus (Thermo Fisher Scientific). Each reaction mixture (20 μL) was composed of 10 μL of SYBR premix Ex Taq I or II, 1 μL of each primer (Key resources table.10 pmol/μL), 4 μL of the DNA template, and 4 μL of distilled water. The amplification reaction was performed using primers (total 16S rRNA gene, Key resources table) with one cycle at 95 °C for 30 s, 35 cycles at 95 °C for 30 s followed by 63, 60, or 55 °C for 30 s, and ending the reaction at 72 °C for 50 s. The fluorescent products were detected during the last step of each cycle. Melting curve analysis was performed after amplification to determine the target from the non-targeted PCR product. The melting curves were obtained via slow heating from 65 °C to 95 °C at a rate of 0.5 °C/s.

DNA extraction from the fecal pellet and 16S rRNA gene sequencing

Bacterial DNA was extracted from the feces using an E.Z.N.A® Stool DNA kit (Omega Bio-Tek; GA, USA) and purified using magLEAD 12gc (Precision System Science; Chiba, Japan). PCR was performed using KAPA HiFi HotStart ReadyMix (Nippon Genetics; Tokyo, Japan), and the primer set was used for the V3 to V4 region of the 16S rRNA gene (Key resources table). The amplicons were purified using AMPure XP (Beckman Coulter; CA, USA). DNA from each sample was added to different index sequences using the Nextera XT index kit (Illumina; CA, USA). Mixed samples were prepared by pooling approximately equal amounts of amplified DNA and sequenced using Miseq Reagent Kit V3 (600 Cycle) and a Miseq sequencer (Illumina), in accordance with the manufacturer's instructions.

Sequencing data were analyzed using Qiime2 (version 2020.11) (Bolyen et al., 2019). To trim the primer region from raw sequences, Cutadapt in Qiime2 plugin was used (https://doi.org/10.14806/ej.17.1.200). The sequences without the primer region were processed for quality control, paired-end read joining, chimera filtering, and ASV table construction using the DADA2 algorithm (Callahan et al., 2016). For each ASV representative sequence, BLAST (Pruesse et al., 2007) was used to assign the taxonomy based on the SILVA database (version 138) (Camacho et al., 2009). After random sampling of 10,600 reads using the feature table (Weiss et al., 2017), the compositional data was converted, and diversity analysis was performed.

Preparation of colonic lamina propria cells

Colonic lamina propria cells were prepared using a method described previously (Goodyear et al., 2014) with some modifications. The colons were isolated, opened longitudinally, washed with HBSS (Nacalai Tesque), cut into four segments, and shaken in HBSS containing 10 μM dithiothreitol, 20 mM EDTA, and 12.5 mM HEPES (Nacalai Tesque) at 37 °C for 20 min. After vortexing, the colonic tissues were centrifuged at 70 × *g* for 30 s, and the supernatant was discarded. The tissues were shaken in HBSS containing 20 mM EDTA and 10 mM HEPES at 37 °C for 20 min. The tissues were then minced and dissociated with RPMI1640 (Nacalai Tesque) containing 0.2 U/mL Liberase TM (Roche Diagnostics; Mannheim, Germany), 0.125 mg/mL DNase I (Merck; Darmstadt, Germany), 2% NBCS (Thermo Fisher Scientific), 100 U/mL penicillin, 100 μg/mL

streptomycin (Nacalai Tesque), and 20 mM HEPES at 37 °C for 30 min to obtain single-cell suspensions. After filtering, the single-cell suspensions were washed with HBSS and subjected to flow cytometry analysis.

Flow cytometry

Colonic lamina propria cells were incubated with anti-mouse CD16/CD32 antibody (93; BioLegend; CA, USA) to block Fc receptors and then stained using antibodies conjugated with Brilliant Violet 421, BV510 (BV), Alexa Fluor 488, phycoerythrin (PE), PE-CF594, PE-Cy7, allophycocyanin (APC), or APC-Cy7. CD45 (30-F11), F4/80 (BM8), Siglec-F (E50-2440), CD4 (GK1.5), CD11c (6D5), CD45R/B220 (RA3-6B2), Ly6C (AL-21), and TCRβ (H57-597) antibodies were obtained from BioLegend. CD11b (M1/70) and CD4 (GK1.5) antibodies were obtained from (Thermo Fisher Scientific). Ly6G (1A8), Siglec-F (E50-2440), Ly6C (AL-21), and CD45R/B220 (RA3-6B2) antibodies were obtained from BD Biosciences. The compound, 7-AAD (BioLegend) or Fixable Viability Stain 780 (BD Biosciences) was added to the cell suspension to label dead cells. The stained cells were analyzed using MACSQuant (Miltenyi Biotec, Bergisch Gladbach, Germany).

IC-MS-based metabolomic analysis of intracellular bacterial metabolites

Frozen bacterial pellets along with internal standard compounds (see below) were sonicated in ice-cold methanol (500 μL) and added to an equal volume of chloroform and 0.4 volume of ultrapure water (LC/MS grade, Wako). The suspension was centrifuged at 15,000 × *g* for 15 min at 4 °C. After centrifugation, the aqueous phase was subjected to ultrafiltration using an ultrafiltration tube (Ultrafree MC-PLHCC, Human Metabolome Technologies). The filtrate was concentrated using a vacuum concentrator (SpeedVac, Thermo). The concentrated filtrate was dissolved in 50 μL ultrapure water and used for IC-MS analysis.

Methionine sulfone and 2-morpholinoethanesulfonic acid were used as internal standards for cationic and anionic metabolites, respectively. Loss of endogenous metabolites during sample preparation was corrected by calculating the recovery rate (%) of the standards in each sample measurement. Metabolites were measured using an orbitrap-type MS (Q-Exactive focus; Thermo Fisher Scientific) connected to a high-performance ion-chromatography (IC) system (ICS-5000+, Thermo Fisher Scientific) that enables highly selective and sensitive metabolite quantification owing to the IC-separation and Fourier Transfer MS principle (Hu et al., 2015). The IC was equipped with an anion electrolytic suppressor (Thermo Scientific Dionex AERS 500) to convert the potassium hydroxide gradient into pure water before the sample entered the mass spectrometer. The separation was performed using a Thermo Scientific Dionex IonPac AS11-HC, 4-μm particle size column. The IC flow rate was set to 0.25 mL/min, which was supplemented post-column with 0.18 mL/min makeup flow of MeOH. The potassium hydroxide gradient conditions for IC separation were set as follows: from 1 mM to 100 mM (0–40 min), 100 mM (40–50 min), and 1 mM (50.1–60 min), at a column temperature of 30 °C. The Q Exactive Focus mass spectrometer was operated under an ESI negative mode for all analyses. A full mass scan (m/z 70–900) was performed at a resolution of 70,000. The automatic gain control target was set at 3×10^6 ions, and the maximum ion injection time was set at 100 msec. Source ionization parameters were optimized with the spray voltage of 3 kV, and other parameters were set as follows: transfer temperature = 320 °C, S-Lens level = 50, heater temperature = 300 °C, Sheath gas = 36, and Aux gas = 10.

Statistical analyses

Statistical analyses were performed using GraphPad Prism software version 8.3.0 (GraphPad Software Inc.). For evaluation of differences between two groups, we performed the Shapiro-Wilk normality to assess whether to use parametric or nonparametric statistics. If the data were parametric, we conducted F-test to identify whether there are equal variances, followed by unpaired Student's t-test or Welch's t-test. If the data were nonparametric, we conducted Mann-Whitney U-test. For evaluation of differences among more than two groups, we performed the Shapiro-Wilk normality test to assess whether to use parametric or nonparametric statistics. If the data were parametric, we conducted Bartlett's test to identify whether there are equal variances, followed by one-way ANOVA or two-way ANOVA with Tukey's multiple comparison test, Dunnett's multiple comparison test, or Sidak's corrections for multiple comparisons. If the data were nonparametric, we conducted Dunn's multiple comparisons test.